A Comparison of Linear Guidance Techniques, Applied to a Low-Thrust Orbit Transfer Problem

Thesis by

Pieter Wilhelm Stoker

In Partial Fulfillment of the Requirements
for the degree of
Mechanical Engineer

California Institute of Technology
Pasadena, California

1975

(Submitted May 16, 1975)

ACKNOWLEDGMENTS

The author wishes to express his appreciation to his advisor, Professor Thomas K. Caughey, for the encouragement and the advice he has offered during the course of this study. He would also like to express his appreciation to Professors Homer J. S. Stewart and Donald E. Hudson for serving on the supervising committee and Dr. Lincoln J. Wood for his advice and helpful suggestions.

Finally, the author wishes to thank the Department of Mechanical Engineering for computer time and the South-African Council for Scientific and Industrial Research for granting the scholarship that made this study possible.

ABSTRACT

The problem considered is that of a three-dimensional, minimum time, heliocentric, Earth-Mars transfer of a continuous low-thrust rocket vehicle.

The first order necessary conditions of the calculus of variations define the optimal trajectory in terms of a nonlinear first order two-point boundary-value problem, which is solved by the backward-sweep method. The calculation of a set of feedback gain matrices, a cross-check on the numerical accuracy of these matrices, and the satisfaction of a set of necessary conditions for the trajectory to be at least locally minimizing are done simultaneously.

The spacecraft is then perturbed from the nominal trajectory, and two neighboring optimum feedback control laws, the so-called time-to-go guidance technique, and minimum distance guidance technique are compared.

In-plane and out-of-plane perturbations are considered, and both guidance techniques, in most cases, reduce the initial error, although not by a very large factor.

It is shown that the minimum distance technique, as applied in this study, performs much better than found by Lattimore.[1]

---

[1] Lattimore, J. P. "A Comparison of Open and Closed Loop Applications of the Minimum Distance Guidance Technique," University of Texas at Austin, Engineer's Degree Dissertation, 1972.

LIST OF FIGURES

Figure		Page
1	Coordinate System and Control Angles	7
2	Parameters Associated with Time-To-Go Guidance	27
3	Parameters Associated with Minimum Distance Guidance	29
4	Terminal Velocity Error for an Initial Perturbation in x_1 Velocity, Introduced at Zero Days	50
5	Terminal Position Error for an Initial Perturbation in x_1 Velocity, Introduced at Zero Days	51
6	Terminal Velocity Error for an Initial Perturbation in x_4 Position, Introduced at Zero Days	52
7	Terminal Position Error for an Initial Perturbation in x_4 Position, Introduced at Zero Days	53
8	Terminal Velocity Error for an Initial Perturbation in x_3 Velocity, Introduced at Zero Days	54

LIST OF FIGURES (CONTINUED)

Figure		Page
9	Terminal Position Error for an Initial Perturbation in x_3 Velocity, Introduced at Zero Days	55
10	Terminal Velocity Error for an Initial Perturbation in x_6 Position, Introduced at Zero Days	56
11	Terminal Position Error for an Initial Perturbation in x_6 Position, Introduced at Zero Days	57

TABLE OF CONTENTS

	Page
Acknowledgment	ii
Abstract	iii
List of Figures	iv
Chapter 1 - Introduction	1
1.1 The Guidance Problem	1
1.2 Motivation for the Investigation	3
1.3 Notation Convention	4
Chapter 2 - The Optimal Trajectory	6
2.1 The Three-Dimensional Mathematical Model and Coordinate System	6
2.2 Equations of Motion	8
2.3 Necessary and Sufficient Conditions for a Locally Minimizing Time Optimal Reference Trajectory	10
Chapter 3 - Numerical Solution of the Transfer Problem and a Set of Feedback Gains	18
3.1 Several Algorithms	18
3.2 A Backward Sweep Algorithm	20
3.3 Numerical Aspects	21
3.4 A Cross Check on the Accuracy of the Feedback Gains	22
Chapter 4 - Two Different Linear Guidance Schemes	25
4.1 The Time-To-Go Guidance Technique	26
4.2 The Minimum Distance Guidance Technique	30

TABLE OF CONTENTS (CONTINUED)

Page

4.3 Minimum Distance and Time-To-Go Guidance - Previous Results 31

4.4 Minimum Distance and Time-To-Go Guidance - The Algorithms Used in This Study 37

Chapter 5 - Results of the Simulations 39

5.1 Numerical Problems Encountered in Implementing the Guidance Schemes 39

5.2 Results of the Flight Simulations 43

5.3 A Second Minimum Distance Guidance Technique 47

Appendices

Appendix 1 - Earth Orbital Data, Mars Orbital Data, and Other Constants 66

Appendix 2 - Initial Conditions 67

Appendix 3 - Equations Used in This Study 68

Appendix 4 - Feedback Gain Matrices 77

Bibliography 82

CHAPTER 1

INTRODUCTION

Since the appearance of the high speed digital computer, the solution of trajectory optimization problems has been a subject of extensive research. The solution of any of these problems, even on modern computers, is very time consuming. In certain trajectory problems, for instance re-entry flights, this is an important factor. As a result, research was also directed to perturbation guidance - a procedure which gives information about the control history if the spacecraft is, for some reason, perturbed from the precalculated optimal trajectory. In order to determine the relative merits of several perturbation guidance schemes, the low-thrust transfer problem has received much attention in the literature.[1, 2, 4, 6] This example is of theoretical interest only, since in real missions there is in most cases enough time to re-optimize the trajectory in case a disturbance should occur. Nevertheless, some interesting facts have crystallized out of the various low-thrust studies made.

1.1 The Guidance Problem

The nonlinear ordinary differential equation that describes the motion of an interplanetary spacecraft can be expressed as:

$$\dot{\underline{x}}(t) = \underline{f}[\underline{x}(t), \underline{u}(t), t] , \qquad (1.1.1)$$

where $\underline{x}$ is a n vector of state variables, $\underline{u}$ is a m vector of control variables, $\underline{f}$ is a known n vector function, and t is the independent variable, time.

A nominal control history, say $\underline{u}_N(t)$, that will minimize a scalar performance index of the form

$$J = \int_{t_o}^{t_f} 1 \cdot dt \,, \qquad (1.1.2)$$

while satisfying q terminal constraints of the form

$$\underline{Y}[\underline{x}(t_f), t_f] - \underline{y} = 0 \,, \qquad (1.1.3)$$

must be found. The initial time and state are specified and the final time, t_f, is allowed to vary. $\underline{y}$ is a vector of constants.

A set of necessary conditions generates the solution to the above problem, while a set of sufficient conditions guarantees that the resulting state history is at least locally minimized.

Once the mission is initiated, small disturbances that will place the spacecraft off the precalculated path are likely to occur. The resulting variations in the state vector are represented as:

$$\delta\underline{x}(t) = \underline{x}(t) - \underline{x}_N(t) \,, \qquad (1.1.4)$$

where $\underline{x}(t)$ represents the perturbed state and the subscript N denotes the nominal (precalculated) state.

If such a state error is detected, the perturbation guidance program calculates a control variation history which will, if added to the nominal control history, still minimize the transfer time, while satisfying the terminal constraints. Of the most widely used perturbation guidance algorithms are time-to-go guidance and minimum distance guidance.

Perfect knowledge of all state variables of the problem considered in this study is assumed so that the control problem is deterministic.

1.2 Motivation for the Investigation

Hart[1] made a comparison between time-to-go guidance, minimum distance guidance, and several other guidance techniques. The comparison example was a three-dimensional, minimum time, heliocentric, Earth-Mars transfer of a continuous low-thrust rocket vehicle. In this work it was concluded that time-to-go guidance exhibits a poor performance in minimizing the terminal constraint errors. The time-to-go algorithm was applied in an open loop fashion, and the problem considered was that of a rendezvous.

Wood[4, 6] considered a two-dimensional, Earth to Mars orbit transfer and concluded that time-to-go handles even very large initial errors quite well. It was attempted to rendezvous with the orbit of Mars rather than with the planet itself. The problem therefore is less constrainted. Also, the time-to-go algorithm was presented in a closed loop fashion.

The large discrepancy between Wood's study - where a large initial perturbation resulted in a small terminal error - and Hart's study - where a small initial perturbation resulted in a large terminal error - promoted this study.

In this study, it will be attempted to apply the time-to-go algorithm presented in Ref. [11] to Hart's problem in an attempt to develop an understanding of this discrepancy. Endeavoring to attain a smaller terminal error than that found by Lattimore,[2] the minimum distance algorithm as presented by Lattimore[2] will also be applied. The nominal trajectory will be calculated by a backward-sweep algorithm. This algorithm simultaneously generates a set of feedback gain matrices. This procedure when compared to the transition-matrix algorithm (as used by Hart) often has a greater numerical accuracy, since unit solutions of the second-order influence equations may differ by orders of magnitude, producing an ill-conditioned transition matrix.[5]

1.3 Notation Convention

All vectors are assumed to be column vectors and will be denoted by lower case letters; i.e., $\underline{x}, \underline{\lambda}$. Vector components will be denoted by a subscript, i.e., x_1, λ_4. A superscript T denotes the transpose of a matrix, and the superscript -1 indicates the inverse of a square matrix.

The first partial derivative of a scalar with respect to a vector is a row vector denoted by

$$\frac{\partial H}{\partial \underline{x}} = H_{\underline{x}} = \left(\frac{\partial H}{\partial x_1} \; \frac{\partial H}{\partial x_2} \cdots\cdots \frac{\partial H}{\partial x_n} \right).$$

Second partial derivatives of scalars with respect to vectors are matrices denoted by

$$\frac{\partial^2 H}{\partial \underline{u} \partial \underline{x}} = \left[\frac{\partial}{\partial \underline{u}} \left(\frac{\partial H}{\partial \underline{x}} \right)^T \right] = H_{\underline{x}\underline{u}} = \begin{bmatrix} H_{x_1 u_1} & \cdots & H_{x_1 u_m} \\ \vdots & & \vdots \\ H_{x_n u_1} & \cdots & H_{x_n u_m} \end{bmatrix}.$$

First partial derivatives of vectors, with respect to vectors, are also matrices:

$$\frac{\partial \underline{f}}{\partial \underline{x}} = \underline{f}_{\underline{x}} = \begin{bmatrix} \frac{\partial f_1}{\partial x_1} & \cdots & \frac{\partial f_1}{\partial x_n} \\ \vdots & & \vdots \\ \frac{\partial f_n}{\partial x_1} & \cdots & \frac{\partial f_n}{\partial x_n} \end{bmatrix} .$$

The variation of (*) is denoted by δ(*), and the differential of (*) is denoted by d(*). ($\dot{*}$) denotes $\frac{d}{dt}$(*).

CHAPTER 2

THE OPTIMAL TRAJECTORY

After the definition of the mathematical model and coordinate system, a very brief summary is given of all the necessary and sufficient conditions which must be satisfied in order to obtain the solution to the control problem. For details of the derivations, see Refs. [5, 6].

2.1 The Three-Dimensional Mathematical Model and Coordinate System

In this study the mathematical model, coordinate system, initial conditions, and vehicle constants were chosen exactly as in Refs. [1, 2].

The equations of motion, which describe the minimum time low-thrust, heliocentric, Earth-to-Mars transfer, are expressed in terms of a heliocentric, rectangular, coordinate system, x_4, x_5, x_6. The origin of the coordinate system coincides with the Sun, and the x_4 axis coincides with the line of the ascending node of Mars. The x_4 and x_5 axes lie in the ecliptic plane. The x_6 axis coincides with the angular momentum vector of the Earth w.r.t. the Sun. See Figure 1.

The spacecraft is represented by a point mass under the influence of only the central force of the Sun and that of a constant (magnitude) low-thrust jet.

In the beginning of the mission, the gravitational effects of the Earth are neglected. Instead, the spacecraft is given the

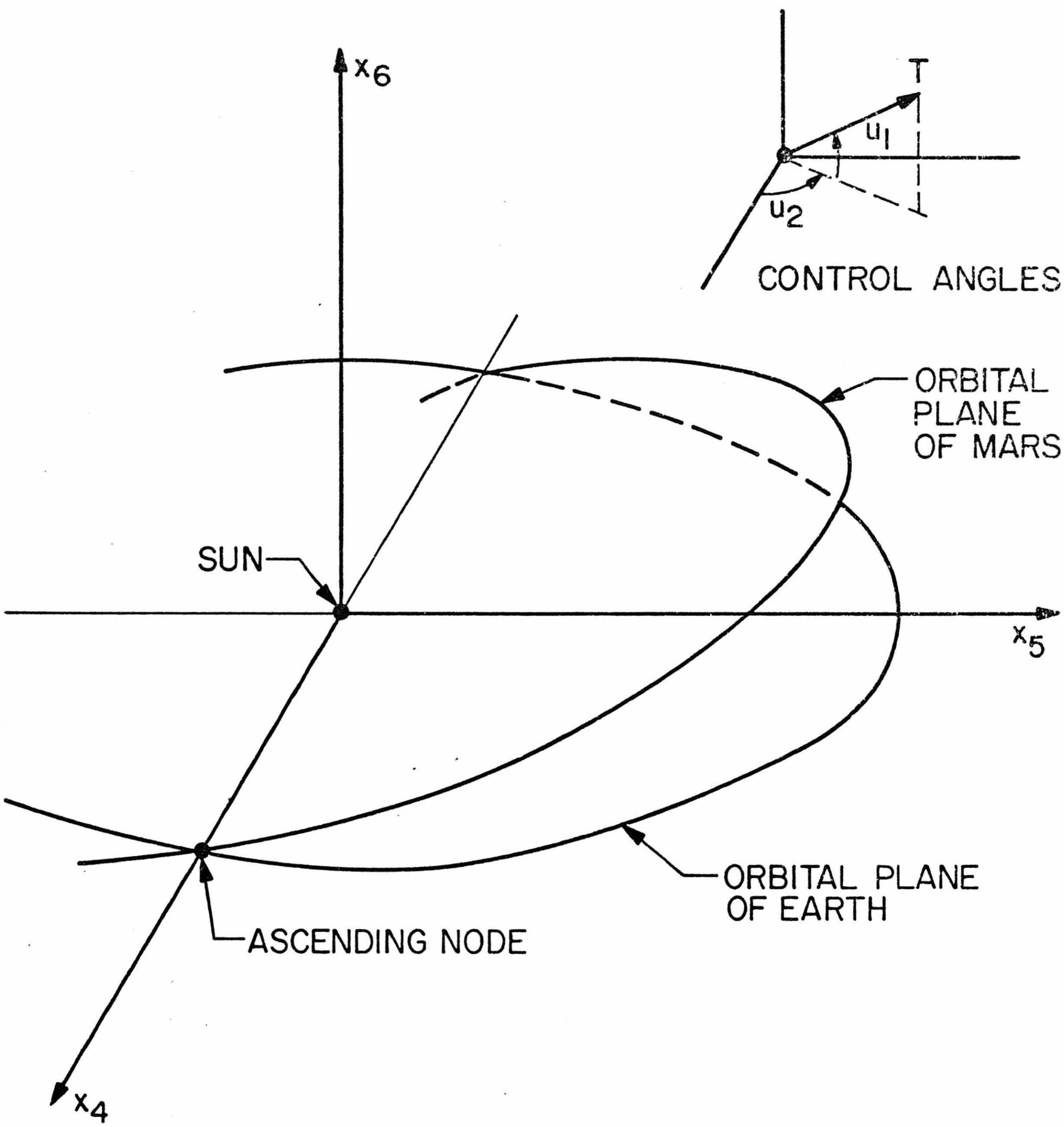

FIGURE 1

Coordinate System and Control Angles

position and velocity of the Earth at the initial time.[13] These initial conditions are given in Appendix 2.

At the end of the mission, the gravitational effects of Mars are also neglected. Along the trajectory, the perturbing effects of other planets were ignored. The inclusion of such forces would complicate the analysis considerably and would make interpretation of results much more difficult.

Information on the orbits of the Earth and Mars can be found in Appendix 1. For the coordinate system employed, the angle of the ascending node of Mars is taken to be 0.0 rad.

Finally, note that we want to rendezvous with Mars.

2.2 Equations of Motion

By a straightforward application of Newtons law, the equations of motion for the space vehicle in the three-dimensional reference frame are given by the following set of first-order, non-linear, ordinary, differential equations:

$$\begin{aligned}
\dot{x}_1 &= \frac{-\mu x_4}{r^3} + \frac{T}{m}\cos u_1 \cos u_2 \\
\dot{x}_2 &= \frac{-\mu x_5}{r^3} + \frac{T}{m}\cos u_1 \sin u_2 \\
\dot{x}_3 &= \frac{-\mu x_6}{r^3} + \frac{T}{m}\sin u_1 \\
\dot{x}_4 &= x_1 \\
\dot{x}_5 &= x_2 \\
\dot{x}_6 &= x_3 \\
r^2 &= x_4^2 + x_5^2 + x_6^2
\end{aligned} \qquad (2.2.1)$$

$$T = \beta \cdot C ,$$
$$m = m_o - \beta t , \qquad (2.2.1 \text{ cont.})$$

where x_1, x_2, x_3 are the velocity components of the spacecraft, x_4, x_5, x_6 are the corresponding position coordinates, μ is the gravitational constant of the Sun, r is the distance of the spacecraft from the Sun, and T is the magnitude of the thrust vector. The angles, u_1 and u_2 describe the direction of the thrust vector, β is the constant mass ejection rate, C is the constant relative speed of the exhaust gas, m_o is the initial mass of the spacecraft, including fuel, and t is the independent variable, time.

Numerical values for the constants β, m_o, C, and μ can be found in Appendix 1.

The six initial conditions for the above mentioned set of differential equations are

$$\underline{x}(t_o) - \underline{x}_E(t_o) = \underline{0} ,$$

where $\underline{x}_E$ is a six column vector representing the state of the Earth at the initial time t_o. Numerical values for $\underline{x}_E(t_o)$ are given in Appendix 2.

Since a rendezvous problem is considered, there are six terminal constraints, denoted by

$$\underline{Y}[\underline{x}(t_f), t_f] - \underline{y} = \underline{x}(t_f) - \underline{x}_M(t_f) , \qquad (2.2.2)$$

where t_f is the terminal time, $\underline{y}$ is a vector of constants, $\underline{Y}$ is a six vector function of terminal constraint relations, and $\underline{x}_M$

represents the state of Mars. Note that for the transfer problem $\underline{y} = 0$. The details of the constraint relations (2.2.2) can be found in Appendix 3.

2.3 Necessary and Sufficient Conditions for a Locally Minimizing Time Optimal Reference Trajectory

The problem of finding the control history that will minimize (at least locally) the transfer time while meeting the terminal constraints can formally be stated as follows: Find the n-dimensional set of state variable functions $\underline{x}(t)$ and m-dimensional control variable functions $\underline{u}(t)$ that satisfy a set of n ordinary differential equations of the form

$$\dot{\underline{x}}(t) = \underline{f}(\underline{x}, \underline{u}, t), \quad t_0 \le t \le t_f, \quad \underline{x}(t_0) \text{ given,} \tag{2.3.1}$$

and $q \le n$ terminal constraint relations of the form

$$\underline{Y}[\underline{x}(t_f), t_f] - \underline{y} = 0, \tag{2.3.2}$$

while minimizing a scalar performance index of the form

$$J = g[\underline{x}(t_f), t_f] + \int_{t_0}^{t_f} L(\underline{x}, \underline{u}, t)\, dt. \tag{2.3.3}$$

The final time is unspecified.

The functions $\underline{f}$, L, $\underline{Y}$, and g are twice continuously differentiable with respect to their arguments.

By using the classical calculus of variations approach, a set of conditions which are necessary and sufficient to guarantee weak minimization of the above performance index, while satisfying the constraint relations, is given by:[3-6]

2.3.a Necessary Conditions

$$\dot{\underline{x}} = \underline{f}(\underline{x}, \underline{u}, t) , \qquad t_o \leq t \leq t_f \tag{2.3.4a}$$

$$\dot{\underline{\lambda}}^T = -H_{\underline{x}} , \qquad t_o \leq t \leq t_f \tag{2.3.4b}$$

$$\underline{0} = H_{\underline{u}} , \qquad t_o \leq t \leq t_f \tag{2.3.4c}$$

$$t_o,\ \underline{x}(t_o) \text{ specified,} \tag{2.3.4d}$$

$$\underline{Y}(\underline{x}_f, t_f) - \underline{y} = 0 , \tag{2.3.4e}$$

$$\underline{\lambda}^T(t_f) = G_{\underline{x}_f} , \tag{2.3.4f}$$

$$z(\underline{x}_f, \underline{u}_f, t_f, \underline{v}) \triangleq \left(L + \frac{dG}{dt_f}\right)_{t=t_f} = 0 . \tag{2.3.4g}$$

G, H, $\underline{v}$, and $\underline{\lambda}$ are defined in paragraph 2.3.b.

The above set of equations defines an extremal path. If we consider small perturbations in the initial state $\delta\underline{x}(t_o)$ and in the terminal conditions $d\underline{y}$, these perturbations will give rise to perturbations $\delta\underline{x}(t)$, $\delta\underline{\lambda}(t)$, and $\delta\underline{u}(t)$. It can be shown[5] that these perturbations satisfy

$$\delta\dot{\underline{x}} = A(t)\,\delta\underline{x} - B(t)\,\delta\underline{\lambda} , \tag{2.3.5a}$$

$$\delta\dot{\underline{\lambda}} = -C(t)\,\delta\underline{x} - A^T(t)\,\delta\underline{\lambda} , \tag{2.3.5b}$$

$$\delta\underline{u}(t) = -H_{\underline{u}\,\underline{u}}^{-1}\left(H_{\underline{u}\,\underline{x}}\,\delta\underline{x} + \underline{f}_{\underline{u}}^T\,\delta\underline{\lambda}\right) , \tag{2.3.5c}$$

where

$$A(t) = \underline{f}_{\underline{x}} - \underline{f}_{\underline{u}} H_{\underline{u}\underline{u}}^{-1} H_{\underline{u}\underline{x}} , \tag{2.3.6a}$$

$$B(t) = \underline{f}_{\underline{u}} H_{\underline{u}\underline{u}}^{-1} \underline{f}_{\underline{u}}^{T} , \tag{2.3.6b}$$

$$C(t) = H_{\underline{x}\underline{x}} - H_{\underline{x}\underline{u}} H_{\underline{u}\underline{u}}^{-1} H_{\underline{u}\underline{x}} . \tag{2.3.6c}$$

2.3.b Sufficient Conditions

$H_{\underline{u}\underline{u}}(t)$ positive definite , $t_0 \le t \le t_f$ (2.3.7a)

$\underset{\sim}{S}_*(t)$ finite for $t_0 \le t \le t_1$, and $\underset{\sim}{S}(t)$ finite for $t_1 \le t \le t_f$, where t_1 is any intermediate time such that $t_0 \le t_1 \le t_f$. Alternatively, we must have $\underset{\sim}{S}_*(t)$ finite for $t_0 \le t \le t_f$, except at t_f where it need not exist. (2.3.7b)

$\frac{dz}{dt_f} > 0$, applicable only in cases where $\frac{d\underline{Y}}{dt_f} = 0$ (2.3.7c)

Note that we have used the notation $\underline{x}_f$ for $\underline{x}(t_f)$.

The quantities G and H are defined by introducing a set of n undetermined time dependent multipliers $\underline{\lambda}(t)$ and a set of q constant multipliers $\underline{v}$ as follows:

$$G(\underline{x}_f, t_f, \underline{v}) = g + \underline{v}^T \underline{Y} \tag{2.3.8}$$

$$H(\underline{x}, \underline{u}, \underline{\lambda}, t) = L + \underline{\lambda}^T \underline{f} \tag{2.3.9}$$

The sweep matrices $\underset{\sim}{S}(t)$, $\underset{\sim}{R}(t)$, $\underset{\sim}{Q}(t)$, $\underset{\sim}{S}_*(t)$, $\underset{\sim}{R}_*(t)$, and $\underset{\sim}{Q}_*(t)$ are defined by the following set of differential equations and boundary conditions:

$$\dot{S} = -A^T S - SA + SBS - C , \qquad (2.3.10a)$$

$$\dot{R} = (SB - A^T)R , \qquad (2.3.10b)$$

$$\dot{Q} = R^T B R , \qquad (2.3.10c)$$

$$S(t_f) = G_{\underline{x}_f \underline{x}_f} , \qquad (2.3.11a)$$

$$R(t_f) = [\underline{Y}_{\underline{x}_f}^T \quad z_{\underline{x}_f}^T] , \qquad (2.3.11b)$$

$$Q(t_f) = \begin{bmatrix} 0 & \frac{d\underline{Y}}{dt_f} \\ \left(\frac{d\underline{Y}}{dt_f}\right)^T & \frac{dz}{dt_f} \end{bmatrix} , \qquad (2.3.11c)$$

$$S_* = S - RQ^{-1}R^T , \qquad (2.3.12a)$$

$$R_* = RQ^{-1} , \qquad (2.3.12b)$$

$$Q_* = -Q^{-1} , \qquad (2.3.12c)$$

where A(t), B(t), and C(t) are defined in paragraph 2.3.a.

Note that the $(\ )_*$ quantities also satisfy (2.3.10).

In Ref. [6] it is shown that if the first order necessary conditions are linearized about the stationary path, neighboring stationary paths are found, characterized by the perturbation equations:

$$\begin{bmatrix} \delta \underline{\lambda}(t) \\ -d\underline{\nu} \end{bmatrix} = \begin{bmatrix} S_*(t) & R_*(t) \\ R_*^T(t) & Q_*(t) \end{bmatrix} \begin{bmatrix} \delta \underline{x}(t) \\ d\underline{\nu} \end{bmatrix} , \qquad (2.3.13)$$

$$\delta u = C_1 \delta \underline{x} + D \delta \underline{\nu} ,$$

where the feedback gain matrices C_1 and D are given by

$$C_1 = -H_{\underline{u}\underline{u}}^{-1} (H_{\underline{u}\underline{x}} + \underline{f}_{\underline{u}}^T \underset{\sim}{S}_*) , \qquad (2.3.14b)$$

$$D = -H_{\underline{u}\underline{u}}^{-1} \underline{f}_{\underline{u}}^T \underset{\sim}{R}_* d\bar{\underline{y}}, \qquad (2.3.14c)$$

and

$$d\bar{\underline{v}} = \begin{bmatrix} d\underline{v} \\ dt_f \end{bmatrix} , \qquad (2.3.15)$$

$$d\bar{\underline{y}} = \begin{bmatrix} d\underline{y} \\ 0 \end{bmatrix} . \qquad (2.3.16)$$

It is sometimes necessary to write (2.3.13) in different forms. The following forms are equivalent to (2.3.13).

$$\begin{bmatrix} \delta\underline{\lambda}(t) \\ d\underline{y} \\ dz \end{bmatrix} = \begin{bmatrix} S(t) & R(t) & \underline{m}(t) \\ R^T(t) & Q(t) & \underline{n}(t) \\ \underline{m}^T(t) & \underline{n}^T(t) & a(t) \end{bmatrix} \begin{bmatrix} \delta\underline{x}(t) \\ d\underline{v} \\ dt_f \end{bmatrix} , \qquad \begin{matrix} (2.3.17a) \\ (2.3.17b) \\ (2.3.17c) \end{matrix}$$

where S, R, $\underline{m}$, $\underline{n}$, and a satisfy the differential equations

$$\dot{S} = -SA - A^T S + SBS - C , \qquad (2.3.18a)$$

$$\dot{R} = -(A^T - SB)R , \qquad (2.3.18b)$$

$$\dot{Q} = R^T B R , \qquad (2.3.18c)$$

$$\dot{\underline{m}} = -(A^T - SB)\underline{m} , \qquad (2.3.18d)$$

$$\dot{\underline{n}} = R^T B \underline{m} \qquad (2.3.18e)$$

$$\dot{a} = \underline{m}^T B \underline{m} , \qquad (2.3.18f)$$

with boundary conditions given by

$$\begin{bmatrix} \delta\underline{\lambda}(t_f) \\ \\ d\underline{y} \\ \\ dz \end{bmatrix} = \begin{bmatrix} G_{\underline{x}_f\underline{x}_f} & (\underline{Y}_{\underline{x}_f})^T & (z_{\underline{x}_f})^T \\ \underline{Y}_{\underline{x}_f} & 0 & \dfrac{d\underline{Y}}{dt_f} \\ z_{\underline{x}_f} & \left(\dfrac{d\underline{Y}}{dt_f}\right)^T & \dfrac{dz}{dt_f} \end{bmatrix} \begin{bmatrix} \delta\underline{x}(t_f) \\ \\ d\underline{v} \\ \\ dt_f \end{bmatrix} . \qquad \begin{matrix} (2.3.19a) \\ (2.3.19b) \\ (2.3.19c) \end{matrix}$$

If $\frac{dz}{dt_f} \neq 0$, Equation 2.3.19c can be solved for dt_f in terms of $\delta\underline{x}(t_f)$ and $d\underline{v}$:

$$dt_f = \left(\frac{dz}{dt_f}\right)^{-1} \left[dz - z_{\underline{x}_f} \delta \underline{x}_f - \left(\frac{d\underline{Y}}{dt_f}\right)^T d\underline{v} \right] . \qquad (2.3.20)$$

Using Equation (2.3.20) in (2.3.19a) and (2.3.19b) we get

$$\begin{bmatrix} \delta\underline{\lambda}(t_f) \\ \\ d\underline{y} \end{bmatrix} = \begin{bmatrix} G_{\underline{x}_f\underline{x}_f} - (z_{\underline{x}_f})^T \left(\dfrac{dz}{dt_f}\right)^{-1} z_{\underline{x}_f} & (\underline{Y}_{\underline{x}_f})^T - \left(\dfrac{d\underline{Y}}{dt_f}\right)^T \left(\dfrac{dz}{dt_f}\right)^{-1} (z_{\underline{x}_f})^T \\ \underline{Y}_{\underline{x}_f} - \dfrac{d\underline{Y}}{dt_f}\left(\dfrac{dz}{dt_f}\right)^{-1} z_{\underline{x}_f} & - \dfrac{d\underline{Y}}{dt_f}\left(\dfrac{dz}{dt_f}\right)^{-1}\left(\dfrac{d\underline{Y}}{dt_f}\right)^T \end{bmatrix} .$$

$$(2.3.21)$$

This elimination makes a simpler backward-sweep possible:

$$\begin{bmatrix} \delta\underline{\lambda}(t) \\ d\underline{y} \end{bmatrix} = \begin{bmatrix} \overline{S}(t) & \overline{R}(t) \\ \overline{R}^T(t) & \overline{Q}(t) \end{bmatrix} \begin{bmatrix} \delta\underline{x}(t) \\ d\underline{v} \end{bmatrix} , \qquad (2.3.22)$$

where

$$\bar{S} = S - \underline{m}\,\underline{m}^T/a \,, \tag{2.3.22}$$

$$\bar{R} = R - \underline{m}\,\underline{n}^T/a \,, \tag{2.3.23}$$

$$\bar{Q} = Q - \underline{n}\,\underline{n}^T/a \,.$$

Note that $\bar{S}$, $\bar{R}$, and $\bar{Q}$ satisfy (2.3.18a, b, c).

Note also that we have partitioned the matrices $\underset{\sim}{R}$, $\underset{\approx}{Q}$, $\underset{\sim}{R}_*$ and $\underset{\approx}{Q}_*$ as follows:

$$\underset{\sim}{R} = [R \quad \underline{m}] \,, \tag{2.3.24a}$$

$$\underset{\sim}{R}_* = [\bar{R}_* \quad \underline{m}_*] \,, \tag{2.3.24b}$$

$$\underset{\approx}{Q} = \begin{bmatrix} Q & \underline{n} \\ \underline{n}^T & a \end{bmatrix} , \tag{2.3.24c}$$

$$\underset{\approx}{Q}_* = \begin{bmatrix} \bar{Q}_* & \underline{n}_* \\ \underline{n}_*^T & a_* \end{bmatrix} , \tag{2.3.24d}$$

$\underline{m}$, $\underline{m}_*$, $\underline{n}$, and $\underline{n}_*$ are column vectors. a and a_* are scalars.

Then from Equations (2.3.13), (2.3.24b), and (2.3.24d), it follows that[4]

$$dt_f = -\underline{m}_*^T(t)\,\delta\underline{x} - \underline{n}_*^T(t)\,d\bar{\underline{y}} \tag{2.3.25}$$

Equations (2.3.4), (2.3.6), and (2.3.11) for the minimum time orbit transfer problem are derived in Appendix 3.

The optimality condition 2.3.4c determines the m-vector $\underline{u}(t)$. The solution to the 2n differential equations (2.3.4a) and (2.3.4b) and the choice of the $q+1$ parameters $\underline{v}$ and t_f are determined by the $2n+q+1$ boundary conditions (2.3.4d) - (2.3.4g).

In the next chapter, an algorithm for the solution of the above two-point boundary-value problem will be presented.

CHAPTER 3

NUMERICAL SOLUTION OF THE TRANSFER PROBLEM AND A SET OF FEEDBACK GAINS

Several algorithms are discussed briefly with particular emphasis on the advantages and disadvantages of each. A detailed discussion of the algorithm selected will then be given, which is followed by some details on the specific integration routine that was used to solve the problem. Some numerical aspects, such as convergence and numerical stability are discussed in paragraph 3.3. Finally, a method which can be used to cross-check the accuracy of the feedback gains is presented.

3.1 Several Algorithms

Several algorithms for the solution of the non-linear, two-point boundary-value problem have been developed {Refs. [5-8] and others}. Among the most well known of these are the neighboring extremal methods, gradient methods and quasilinearization methods.

Except in very special cases, all these methods involve either flooding or iterative procedures.

Gradient methods are in general not very sensitive to initial estimates of the unspecified boundary conditions, and it is therefore a good method to generate a first approximation of the solution. First order gradient methods are, however, slow to converge when the solution approaches the optimal solution, and second order gradient methods are very bulky to program.

Neighboring extremal methods often involve an iterative procedure which improves an initial guess of the unspecified initial (terminal) conditions so as to satisfy the specified terminal (initial) conditions.

The main disadvantage of these methods is the difficulty of finding a first estimate at one end that produces a reasonable solution at the other. This difficulty arises naturally due to the inherent sensitivity of the Euler-Lagrange equations (Eq. 2.3.4b).

Solution by the neighboring extremal method involves the solution of a linear, two-point boundary value problem. Such problems can be solved by either finding a transition matrix between unspecified boundary conditions at one end and specified boundary conditions at the other end, or by a "sweep" method which generates, for the set of equations with specified final conditions, an equivalent set of initial conditions. The coëfficients of the terminal conditions are thus in effect "swept" backwards in time to the initial time. We have then an ordinary initial value problem which is easily integrated. This method involves the integration of a matrix Riccati equation (see Equation 2.3.10a).

As pointed out in Ref. [5], we have, in many systems, a significant difference in the growth of the solutions $\underline{x}(t)$ and $\underline{\lambda}(t)$. Since all calculations are done in finite accuracy, this difference in growth rate often leads to an ill-conditioned transition matrix. The difficulty of an ill-conditioned transition matrix can often be sidestepped by using the "sweep" method.

It is to be noted that handy "by-products" result from the backward-sweep method: If we integrate Equations (2.3.10) backwards with initial conditions (2.3.11) from t_f to t_1, then perform the transformation (2.3.12), and continue the integration to t_o, we can easily calculate a set of feedback gains by using (2.3.14b), while simultaneously investigating the sufficient conditions for a local minimum, (2.3.7b).

Since the solution of the low-thrust Earth-to-Mars transfer in three dimensions was found by Hart[1], there was no starting difficulty, and the backward-sweep method was chosen to generate the solution.

3.2 A Backward Sweep Algorithm[5]

The following algorithm was used to generate the solution to the two-point boundary-value problem stated in Chapter 2.

Step 1: Guess the n terminal conditions $\underline{x}(t_f)$, the q parameters $\underline{v}$, and the terminal time t_f.

Step 2: Determine $\underline{\lambda}(t_f)$ and $z[\underline{x}(t_f), \underline{u}(t_f), \underline{v}, t_f]$ from (2.3.4f) and (2.3.4g). Calculate (2.3.4e).

Step 3: Integrate (2.3.4a) and (2.3.4b) backward from t_f to t_o using (2.3.4c) to determine $\underline{u}(t)$ in terms of $\underline{\lambda}(t)$, with terminal conditions $\underline{x}(t_f)$ and $\underline{\lambda}(t_f)$ from steps 1 and 2.

Step 4: Simultaneously with step 3, integrate (2.3.10) with boundary conditions (2.3.11) to $t = t_1$.

Step 5: At $t = t_1$ carry out the transformation (2.3.12) and continue integration to t_o, using (2.3.10).

Step 6: Record $\underline{x}$, $\underline{\lambda}$, $\underset{\sim}{S}_*$, $\underset{\sim}{R}_*$, $\underset{\sim}{Q}_*$ at $t = t_0$.

Step 7: Choose $\delta\underline{x}(t_0)$, $d\underline{y}$ and dz so as to bring the next solution closer to the desired values of $\underline{x}(t_0)$, $\underline{Y}(\underline{x}_f, t_f) - \underline{y} = 0$ and $z = 0$. A good choice is

$$\begin{bmatrix} \delta\underline{x}(t_0) \\ d\underline{y} \\ dz \end{bmatrix} = -\mathcal{E} \begin{bmatrix} \underline{x}(t_0) - \underline{x}^o \\ \underline{Y}(\underline{x}_f, t_f) - \underline{y} \\ z(\underline{x}_f, t_f) \end{bmatrix}$$ where $\underline{x}^o$ is specified, $0 < \mathcal{E} \leq 1$.

Step 8: Use (2.3.13) and the stored values in step 6 to calculate $\delta\underline{\lambda}(t_0)$ and $d\underline{\overline{v}}$. Record $d\underline{\overline{v}}$.

Step 9: Integrate (2.3.5a, b) forward with boundary conditions $\delta\underline{x}(t_0)$ and $\delta\underline{\lambda}(t_0)$. Record $d\underline{x}(t_f) = \delta\underline{x}(t_f) + \dot{\underline{x}}(t_f)dt_f$.

Step 10: Using

$$\begin{bmatrix} \underline{x}(t_f) \\ \underline{v} \\ t_f \end{bmatrix}_{new} = \begin{bmatrix} \underline{x}(t_f) \\ \underline{v} \\ t_f \end{bmatrix}_{old} + \begin{bmatrix} d\underline{x}(t_f) \\ d\underline{v} \\ dt_f \end{bmatrix},$$

repeat step 1 through 10 until $\underline{x}(t_0) = \underline{x}^o$, $\underline{Y}(x_f, t_f) - \underline{y} = 0$, and $z = 0$ to the desired accuracy.

3.3 Numerical Aspects

In order to speed up the convergence, it was found necessary to perform the elimination discussed in Chapter 2.3.b. This resulted in the simultaneous integration of 90 differential equations instead of the 103 equations obtained from (2.3.4a), (2.3.4b), and

(2.3.10). The boundary conditions for the integration of the 90 differential equations are given by (2.3.4d), (2.3.4f), and (2.3.21).

The above algorithm was programmed and run on an IBM 370/158 computer. It took roughly 4.5 minutes of computation time to simultaneously integrate the 90 differential equations and generate a set of feedback gain matrices at 158 points along the trajectory.

The integration method used is that of R. Bulirsch and J. Stoer. It has a variable step size and uses rational functions rather than polynomials to extrapolate the solution from the discrete approximation.

When compared to Runge Kutta, Adams Moulton Bashforth (of order 6), and methods which extrapolate using polynomials based on the midpoint rule, this method should yield more accurate results and fewer operations to obtain these results. The rational approximation method does not fix the order of approxation, but adapts it automatically to the problem treated.[9]

In highly non-linear regions, the step size was as small as 0.14 days and the maximum step size was limited to 1.7 days. The best time to perform the transformation is approximately 126 days into the mission (taking 0 days as the launching time from the Earth). The solution agrees to within 1% with that of Ref. [1] and it converged within five iterations.

3.4 A Cross Check on the Accuracy of the Feedback Gains[4]

The feedback gain matrix for the transfer problem is given by (see 2.3.14b)

$$C_1(t) = -H_{\underline{u}\,\underline{u}}^{-1} f_{\underline{u}}^T \underset{\sim}{S}^* \tag{3.4.1}$$

It is possible to get an estimate of the accuracy of the feedback gain matrix if an estimate of the accuracy of $\underset{\sim}{S}^*$ can be obtained.

From (2.3.25), it follows that the change in terminal time can be expressed in terms of perturbations in the state and terminal constraint levels by

$$dt_f = -\underline{m}_*^T(t)\,\delta\underline{x}(t) - \underline{n}_*^T(t)\,d\underline{y} . \tag{3.4.2}$$

In addition, if the first order necessary conditions are satisfied, the first variation in the performance index can be expressed as[4]

$$\delta J = \underline{\lambda}^T(t_0)\,\delta\underline{x}(t_0) - \underline{\nu}^T d\underline{y} . \tag{3.4.3}$$

On the nominal path any time t_0 is a possible initial time so that (3.4.3) can be written as

$$\delta J = \underline{\lambda}^T(t)\,\delta\underline{x}(t) - \underline{\nu}^T d\underline{y} . \tag{3.4.4}$$

For the problem under consideration we have $J = \beta t_f$. Hence, from Eqs. (3.4.2) - (3.4.4) we have

$$\begin{aligned} \underline{m}_*(t) &= -\underline{\lambda}(t)/\beta , \\ \underline{n}_*(t) &= \underline{\nu}/\beta = \text{const} . \end{aligned} \tag{3.4.5}$$

For $t_1 \le t \le t_f$, $\underline{m}_*$ is given by the last column of (2.3.12b) which can be evaluated as long as $\underset{\sim}{Q}^{-1}$ exists.

After the transformation, $\underline{m}_*$ can be evaluated by simultaneous backward integration of

$$\dot{\underset{\sim}{S}}_* = -A\underset{\sim}{S}_* - \underset{\sim}{S}_*A + \underset{\sim}{S}_*B\underset{\sim}{S}_* - C ,$$

and (3.4.6)

$$\dot{\underline{m}}_* = -(A^T - B\underset{\sim}{S}_*)\underline{m}_* .$$

Over the first 80% of the integration interval (up to about 155 days from the Earth) the agreement of $\underline{m}_*$ and $\underline{\lambda}/\beta$ was found to be within 2%.

During the last few days a check on $\underline{m}_*$ is not possible since $\underset{\sim}{S}^*$ diverges as t approaches t_f. As t_f is approached, fluctuations in $\underline{m}^*$ increase partly because of large errors introduced by inverting $\underset{\sim}{Q}$, a matrix which is singular at t_f.

The generated feedback gains are given in Appendix 4.

CHAPTER 4

TWO DIFFERENT LINEAR GUIDANCE SCHEMES

In Chapter Two, a method for generating guidance information was discussed. A control correction is obtained from the product of a time dependent feedback gain matrix and a linear state variation. The gain matrices are evaluated along the nominal trajectory and stored as a function of time.

When applying a guidance scheme of this nature, the ambiguity of determining the "lookup" parameter for the gain matrices arises. If, for instance, the spacecraft is perturbed onto a neighboring path such that the final time on the perturbed trajectory is greater than the final time on the nominal trajectory, there are no gain matrices available for the time greater than the nominal final time, so that no guidance information can be calculated. In the event of using the current time on the perturbed trajectory to enter the gain tables, and if there is an index time which represents a nominal state "closer" to the perturbed state, the question arises whether this time should not be used to enter the gain tables.

Several methods exist to circumvent this ambiguity {Refs. [1, 4-6, 10-12, and others]}. In this chapter two of these methods are discussed - the so-called time-to-go technique and the minimum distance technique.

The minimum distance guidance technique employed in this study closely resembles that of Lattimore.[2] The feedback information, however, is calculated in the form of a continuous feedback law, $\delta \underline{u}(t) = C_1(t)\,\delta\underline{x}(t)$, rather than in the form of a sampled data feedback law,[5] $\delta \underline{u}(t) = C_1(t, t_1)\,\delta\underline{x}(t_1)$, as employed by Lattimore. Here t represents the current time on the perturbed trajectory, and t_1 represents the time of the last loop closure.

4.1 The Time-To-Go Guidance Technique

The time-to-go scheme presented in this section avoids the problem of "running out of gains" if the perturbed state of the spacecraft is such that actual t_f is greater than nominal t_f. All the parameters associated with time-to-go are illustrated in Figure 2.

In terms of these parameters, we have

$$T = (t_f - t) = (t_{f_N} - t_N) = \text{time-to-go} \tag{4.1.1a}$$

or

$$t_N = t + (t_{f_N} - t_f) . \tag{4.1.1b}$$

The change in final time can be calculated using Eq. (2.3.25). This method demands the storing of an additional set of feedback gains, namely the Lagrange multipliers, $\underline{\lambda}(t)$.

For problems where the terminal time is allowed to vary, differential changes of $\underline{x}(t)$ and $\underline{u}(t)$ are given by

$$d\underline{x}(t) = \delta\underline{x}(t) + \dot{\underline{x}}(t)\,dt , \tag{4.1.2a}$$

$$d\underline{u}(t) = \delta\underline{u}(t) + \dot{\underline{u}}(t)\,dt , \tag{4.1.2b}$$

to first order in dt. The quantity $\delta(\cdot)$ denotes the variation of $(\cdot)$,

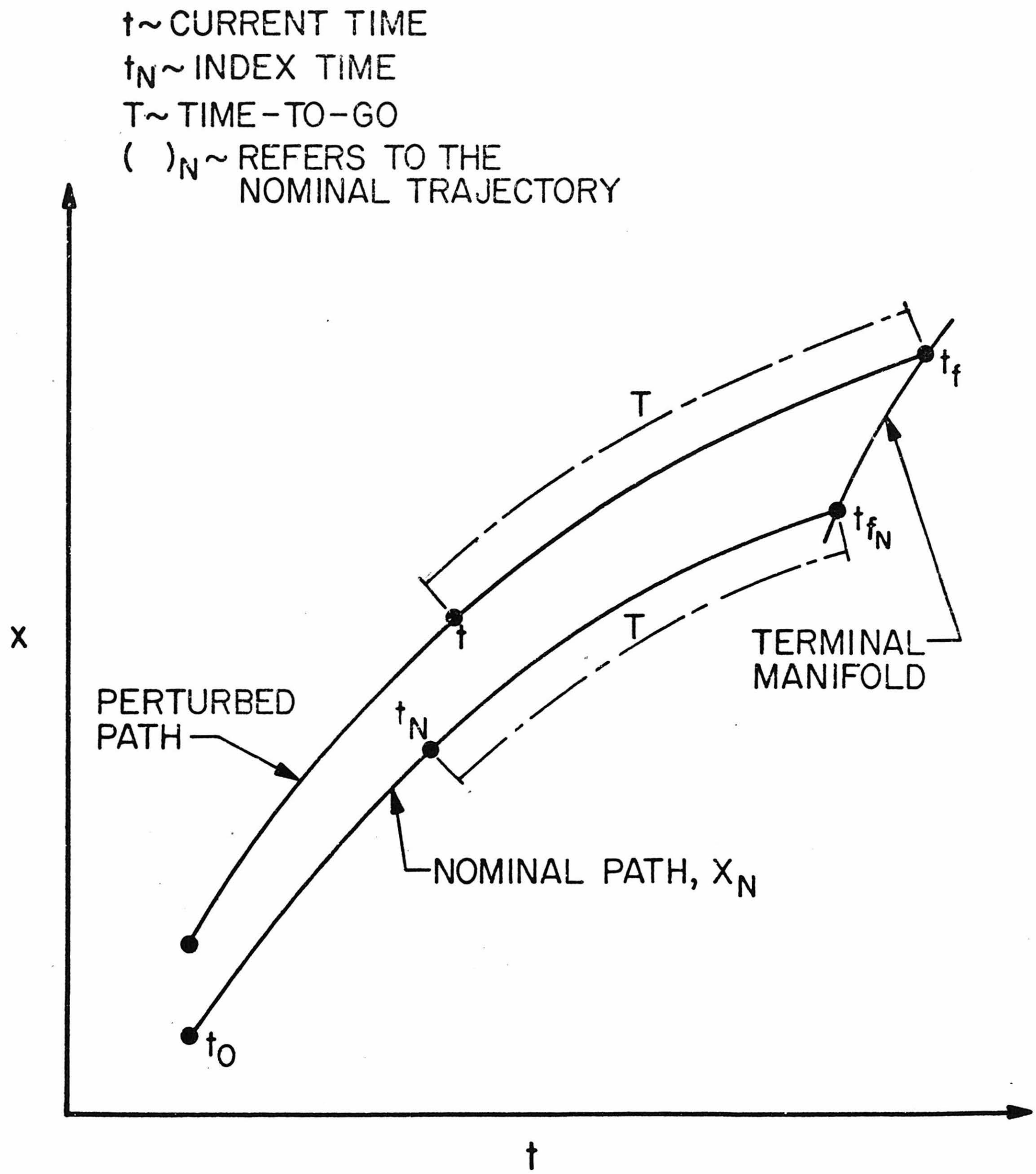

FIGURE 2

Parameters Associated with Time-To-Go Guidance i.e., the change of the quantity at a fixed time t. $d\underline{x}$ and $d\underline{u}$ are defined below.

Using (2.3.25), (4.1.2a), and subtracting dt, the differential of time-to-go is obtained:[4]

$$d(t_f - t) = -\underline{m}_*^T(t)\,d\underline{x}(t) - [1 - \underline{m}_*^T\underline{f}(t)]\,dt - \underline{n}_*^T(t)\,d\bar{\underline{y}} . \quad (4.1.3)$$

The index time, t_N, is then that time t for which $d(t_f - t) = 0$. With such a choice of t_N, (4.1.3) is satisfied to first order in dt.

Using (2.3.14), (4.1.2a, b), and evaluating the gains at t_N, we obtain the feedback law[4]

$$d\underline{u}(t) = C_1(t_N)\,d\underline{x} + [\dot{\underline{u}}(t_N) - C_1(t_N)\underline{f}(t_N)]\,dt + D(t_N)\,d\bar{\underline{y}} , \quad (4.1.4)$$

where

$$C_1(t_N) = -[H_{\underline{u}\underline{u}}^{-1}(H_{\underline{u}\underline{x}} + \underline{f}_{\underline{u}}^T \underset{\sim}{S}_*)]_{t=t_N} , \quad (4.1.5a)$$

$$D(t_N) = -[H_{\underline{u}\underline{u}}^{-1}\underline{f}_{\underline{u}}^T \underset{\sim}{R}_*]_{t=t_N} , \quad (4.1.5b)$$

$$d\underline{u} = \underline{u}(t) - \underline{u}_N(t_N) , \quad (4.1.5c)$$

$$d\underline{x} = \underline{x}(t) - \underline{x}_N(t_N) , \quad (4.1.5d)$$

$$dt = t - t_N , \quad (4.1.5e)$$

$$d\underline{y} = \underline{y} - \underline{y}_N . \quad (4.1.5f)$$

An Algorithm to solve $d(t_f - t) = 0$ is given in Section (4.3). In this study the terminal constraint levels are not varied, that is $d\underline{y} = 0$.

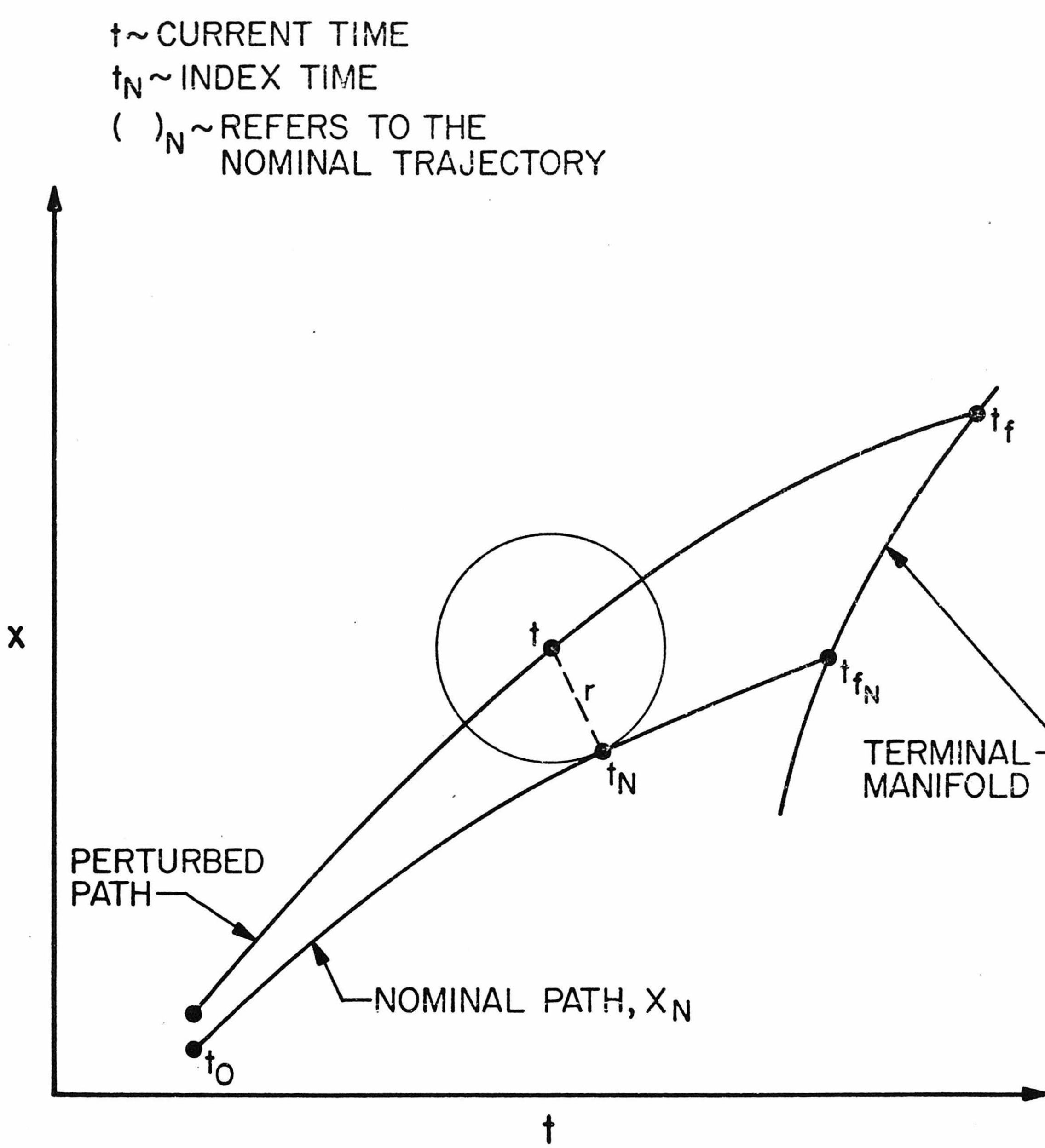

FIGURE 3

Parameters Associated with Minimum Distance Guidance

4.2 The Minimum Distance Guidance Technique

The guidance information used for the minimum distance technique is exactly the same as that used for the time-to-go technique. The schemes differ only in the way this information is used. In the minimum distance technique an index time for entering the gain tables is determined by minimizing a metric function of the difference between the current perturbed state and the nominal trajectory. It is expected that the nominal state "closest" to the perturbed state produces the most accurate feedback data available.[10] The parameters associated with minimum distance guidance are illustrated in Figure 3.

A general form for this metric, as suggested by Powers,[13] is

$$r(\underline{x}, \underline{x}_N, t, t_N) = \{k_0(t - t_N)^2 + k_1[x_1 - x_{N_1}(t)]^2 + \cdots + k_n[x_n - x_{N_n}(t)]\}^{\frac{1}{2}} \tag{4.2.1}$$

where $k_i = k_i(\underline{x})$ is a sensitivity coefficient, generally determined by the physical knowledge of the problem.

Hart[1] and Lattimore[2] considered a special case of (4.2.1) with $k_0 = k_1 = k_2 = k_3 = 0$ and $k_4 = k_5 = k_6 = 1$. Equation (4.2.3) is then obtained by setting

$$\frac{dr}{dt} = [x_4 - x_{N_4}(\tau)]\,\dot{x}_{N_4}(\tau) + [x_5 - x_{N_5}(\tau)]\,\dot{x}_{N_5}(\tau) + [x_6 - x_{N_6}(\tau)]\,\dot{x}_{N_6}(\tau) = 0 \ .$$

Expanding $x_{N_i}(\tau)$ and $\dot{x}_{N_i}(\tau)$ about their values at the current time to first order, that is

$$x_{N_i}(\tau) = x_{N_i}(t) + \dot{x}_{N_i}(t)\Delta t$$
$$\dot{x}_{N_i}(\tau) = \dot{x}_{N_i}(t) + \ddot{x}_{N_i}(t)\Delta t , \qquad i = 4, 5, 6 , \qquad (4.2.2)$$

and solving for Δt:

$$\Delta t = \sum_{i=4}^{6} \left\{ \frac{-\dot{x}_{N_i}(t)[x_i - x_{N_i}(t)]}{\ddot{x}_{N_i}(t)(x_i - x_{N_i}) - \dot{x}_{N_i}(t)^2} \right\} . \qquad (4.2.3)$$

The index time is then given by

$$t_N = t + \Delta t , \qquad (4.2.4)$$

and the change in the control history by

$$\delta \underline{u}(t) = C_1(t_N)\delta \underline{x}(t) , \qquad (4.2.5)$$

where $C_1(t_N)$ is given by (4.1.5a).

Hart[1] and Lattimore[2] used essentially the same law for calculating the control variation. See the introduction of this chapter.

4.3 Minimum Distance and Time-To-Go Guidance - Previous Results

After investigating several open loop guidance algorithms, Hart[1] found that the minimum distance technique is superior to the time-to-go technique. Lattimore[2] continued the investigation of the minimum distance algorithm and applied it in a closed loop form. This study indicated that the closed loop application of the minimum distance algorithm reduces the terminal error only slightly. Furthermore, the terminal error was quite large: for an initial perturbation of 5.0×10^{-6} AU/day in the x_1 velocity component, the Euclidean norm of the terminal velocity errors was approximately 6.81×10^{-3} AU/day.

Since Hart calculated a new optimal trajectory for this perturbed initial condition, the terminal time was uniquely defined. The terminal error was defined as the difference between the state of Mars and the state of the vehicle at this terminal time.

The method applied in this study to calculate the minimum distance index time is that of Lattimore.[2] A different algorithm, however, was used to generate the feedback matrices. For the purpose of comparison, Lattimore's closed loop guidance algorithm will be summarized.

The problem statement, first order necessary conditions, terminal constraint relations, and initial conditions are as in Chapter 2.

Considering a perturbation of the nominal trajectory [Equations (2.3.4a) - (2.3.4c)], and after some algebraic manipulation, one finds

$$\begin{bmatrix} \delta \dot{\underline{x}} \\ \delta \dot{\underline{\lambda}} \end{bmatrix} = \begin{bmatrix} A_1(t) & A_2(t) \\ A_3(t) & A_4(t) \end{bmatrix} \begin{bmatrix} \delta \underline{x} \\ \delta \underline{\lambda} \end{bmatrix} \tag{4.3.1}$$

where

$$A_1(t) = H_{\underline{\lambda}\underline{x}} - H_{\underline{\lambda}\underline{u}} H_{\underline{u}\underline{u}}^{-1} H_{\underline{u}\underline{x}} ,$$

$$A_2(t) = -H_{\underline{\lambda}\underline{u}} H_{\underline{u}\underline{u}}^{-1} H_{\underline{u}\underline{\lambda}} ,$$

$$A_3(t) = -H_{\underline{x}\,\underline{x}} + H_{\underline{x}\,\underline{u}} H_{\underline{u}\,\underline{u}}^{-1} H_{\underline{u}\,\underline{x}} ,$$

$$A_4(t) = -H_{\underline{x}\,\underline{\lambda}} + H_{\underline{x}\,\underline{u}} H_{\underline{u}\,\underline{u}}^{-1} H_{\underline{u}\,\underline{\lambda}} ,$$

with boundary conditions given by (2. 3. 19).

Furthermore,

$$\delta \underline{u} = -H_{\underline{u}\,\underline{u}}^{-1} \{ H_{\underline{u}\,\underline{x}} \delta \underline{x} + H_{\underline{u}\,\underline{\lambda}} \delta \underline{\lambda} \} . \qquad (4.3.2)$$

Numerical integration of (4. 3. 1), using the proper boundary conditions will determine $\delta \underline{x}(t)$ and $\delta \underline{\lambda}(t)$. This is used in (4. 3. 2) to calculate $\delta \underline{u}(t)$. The boundary conditions needed for integrating (4. 3. 1) can be obtained from (2. 3. 19). The $n+q+1$ linearly independent equations (2. 3. 19) contain $2n+q+1$ unknowns $\delta \underline{x}_f$, $\delta \underline{\lambda}_f$, $d\underline{v}$, and dt_f (taking $d\underline{y} = 0$ and $dz = 0$). Choose, therefore, the q components of $d\underline{v}$ and $n-q$ components of $\delta \underline{x}_f$ arbitrarily. The remaining q quantities $\delta \underline{x}_f$ and the $n+1$ quantities $\delta \underline{\lambda}_f$ and dt_f are now uniquely determined and (4. 3. 1) can be integrated backwards in time from t_f to an arbitrary time t_1 in the interval $t_0 \le t_1 \le t_f$.

If the backward integration of (4. 3. 1) is done $n+q$ times with $(n+q)$ linearly independent starting conditions, the $n+q$ solution vectors $\delta \underline{x}$ and $\delta \underline{\lambda}$ forms a $(2n \times n+q)$ transition matrix, denoted by X. Next, partition the transition matrix as:

$$X(t, t_f) = \begin{bmatrix} X_1(t, t_f) & X_2(t, t_f) \\ X_3(t, t_f) & X_4(t, t_f) \end{bmatrix} ,$$

then, after some manipulation, the desired solution for $\delta \underline{x}(t)$ and

$\delta\underline{\lambda}(t)$ is obtained:

$$\begin{bmatrix}\delta\underline{x}(t)\\ \delta\underline{\lambda}(t)\end{bmatrix} = \begin{bmatrix}X_1(t,t_f) & X_2(t,t_f)\\ X_3(t,t_f) & X_4(t,t_f)\end{bmatrix}\begin{bmatrix}X_1(t_1,t_f)^{-1} & -X_1(t_1t_f)^{-1}X_2(t_1t_f)\\ O_{q\times n} & I_{q\times q}\end{bmatrix}\begin{bmatrix}\delta\underline{x}(t_1)\\ d\underline{y}\end{bmatrix}, \tag{4.3.3}$$

where $X_1(t,t_f)$ and $X_3(t,t_f)$ are $n\times n$ matrices and $X_2(t,t_f)$ and $X_4(t,t_f)$ are $n\times q$ matrices.

Finally, Equation (4.3.3) into (4.3.2) gives the control variation history in terms of the state error $\delta\underline{x}(t_1)$ and terminal constraint error $d\underline{y}$.

$$\delta\underline{u}(t) = -[\Lambda_1(t)\ \Lambda_2(t)]$$

$$\begin{bmatrix}X_1(t_1,t_f)^{-1} & -X_1(t_1,t_f)^{-1}X_2(t_1,t_f)\\ O_{q\times n} & I_{q\times q}\end{bmatrix}\begin{bmatrix}\delta\underline{x}(t_1)\\ d\underline{y}\end{bmatrix}, \tag{4.3.4}$$

where

$$\Lambda_1(t) = H_{\underline{u}\,\underline{u}}^{-1}\{H_{\underline{u}\,\underline{x}}X_1(t,t_f) + H_{\underline{u}\,\underline{\lambda}}X_3(t,t_f)\},$$

and

$$\Lambda_2(t) = H_{\underline{u}\,\underline{u}}^{-1}\{H_{\underline{u}\,\underline{x}}X_2(t,t_f) + H_{\underline{u}\,\underline{\lambda}}X_4(t,t_f)\}.$$

Formally then, the algorithm used by Lattimore[2] can be summarized as follows:

Step 1. Solve the $n+q+1$ Equations (2.3.19) $n+q$ times. From the solution of these equations, $n+q$ initial conditions are obtained for the backward integration of Equations (4.3.1).

Step 2. Integrate Equation (4.3.1) $n + q$ times from t_f to t_0 and store the integrated values at each step.

Step 3. Evaluate the gain matrices, $\Lambda_1(t)$ and $\Lambda_2(t)$, using the state of the "closest" point on the nominal trajectory.

Step 4. Substitute $\Lambda_1(t)$ and $\Lambda_2(t)$ into Equation (4.3.4) to obtain the control variation history, $\delta \underline{u}(t)$.

Step 5. Form the augmented control history and integrate the non-linear equations of motion to the time of next loop closure, using the new control history.

Step 6. Evaluate $\delta \underline{x}$ at this time, call it $\delta \underline{x}(t_1)$. If t_1 is less than t_f, go to step 3.

Wood[4, 6] considered a two-dimensional version of the minimum time, low-thrust, Earth to Mars transfer. A rendezvous with Mars is not attempted, instead, it is attempted to match an assumed circular orbit of Mars. A set of feedback gains was generated as described in Chapter 2. After an initial disturbance was introduced, the time-to-go guidance scheme presented in Section 4.1 was used to drive the terminal error to zero. It was concluded that the scheme handles even very large initial perturbations quite well.

After the quantities $\underline{x}$, $\underline{\lambda}$, C_1 and $\dot{\underline{u}} - C_1\underline{f}$ were stored as functions of time, the guidance algorithm used was the following:

Step 1: Assuming the current perturbed state $\underline{x}(t)$ known, obtain the appropriate index time using the algorithm given below.

Step 2. Evaluate the quantities $d\underline{x}$, dt and $d\underline{y}$ and interpolate linearly between the two appropriate data points to obtain $C_1(t_N)$ and other quantities.

Step 3. Calculate $d\underline{u}$ and form the augmented control $\underline{u}(t) = d\underline{u} + \underline{u}_N(t_N)$.

Step 4. Integrate the non-linear equations of motion from t to t + H, where t is the current time and H is the maximum step size.

Step 5. The perturbed state $\underline{x}(t + H)$ is now known. If t + H is less than t_f, go to step 1.

An algorithm for evaluating the index time:

Step 1. Guess a value for the index time and evaluate $d(t_f - t)$ from Equation (4.1.3). A good guess is, for instance, the current time.

Step 2. If $d(t_f - t)$ is greater than zero, choose a smaller value for t_N. If $d(t_f - t)$ is less than zero, choose a larger value for t_N. One might choose, for instance, the index time that coincides with the next/previous data point.

Step 3. Continue the process until $d(t_f - t)$ changes sign, then interpolate linearly between the last two data points to find t_N.

When the initial conditions were such that $d(t_f - t)$ was less than zero when $t_N = t_o$, the index time was chosen to be t_o.

An extensive search in this way was necessary only once. Thereafter the index time can be calculated by two or at most three evaluations of $d(t_f - t)$.

4.4 Minimum Distance and Time-To-Go Guidance - The Algorithms Used in This Study

While generating the nominal trajectory, the 35 quantities $\underline{x}$, $\dot{\underline{x}}$, $\ddot{\underline{x}}$, $\underline{\lambda}$, $\underline{u}$, $(1 - \underline{m}_*^T \underline{f})$, $(\dot{\underline{u}} - C_1\underline{f})$ and C_1 were stored at 158 points. In regions where the control and feedback gains change rapidly, the data points were closer together than in regions where changes in these quantities were small. The minimum time between any two data points was 0.14 days, while the maximum time between any two data points was limited to 1.7 days.

In order to be able to compare the neighboring solution found in this study with that of Lattimore,[2] the terminal constraint levels were not varied.

In applying the minimum distance technique, the index time was determined from Equations (4.2.3) and (4.2.4). The augmented control can then easily be evaluated from Equation (4.2.5).

Formally then, for minimum distance guidance:

Step 1. Assuming the current perturbed state $\underline{x}(t)$ known, use Equations (4.2.3) and (4.2.4) to calculate t_N. Evaluate $\delta\underline{x}(t) = \underline{x}(t) - \underline{x}_N(t)$.

Step 2. Interpolate linearly between the appropriate data points to find $C_1(t_N)$. Evaluate $\delta\underline{u}(t)$ using (4.2.5).

Step 3. Assuming that $\delta\underline{u}(t)$ remains constant over the entire integration step, integrate the non-linear equations of motion forward from t to t+H, using second order interpolation to evaluate the nominal control at any intermediate time $t_H \in [t, t+H]$ and forming the augmented control by adding $\delta\underline{u}(t)$ to this value: $\underline{u}(t) = \delta\underline{u}(t) + u_N(t_H)$. H is the basic step size, i.e., the time between any two data points.

Step 4. The perturbed state $\underline{x}(t+H)$ is now known. If t+H is less than t_f, go to step 1.

The time-to-go guidance algorithm used in this study is the same as the one discussed in Section 4.3, except that steps 3 and 4 in the algorithm of Section 4.3 are replaced by:

Step 3. Calculate $d\underline{u}$ using (4.1.4).

Step 4. Assuming that $d\underline{u}$ stays constant over the step size H, form the augmented control history $\underline{u}(t) = d\underline{u} + \underline{u}_N(t_N + t^1)$, where $0 \le t^1 \le H$, and integrate the non-linear equations of motion forward from t to t+H. Evaluate $\underline{u}_N(t_N + t^1)$ from the stored values of $\underline{u}_N$ by second order interpolation.

Both these algorithms were programmed and various initial perturbations were considered. The results of these flight simulations are discussed in Chapter 5.

CHAPTER 5

RESULTS OF THE SIMULATIONS

The results obtained from the algorithms presented in Chapter 4 are summarized in this chapter. A discussion of some numerical problems encountered in implementing these algorithms and the solutions to these problem areas precedes the results.

5.1 Numerical Problems Encountered in Implementing the Guidance Schemes

A problem area common to both time-to-go and minimum distance guidance is the time period near the end of the flight where the feedback gains diverge. This phenomenon can be explained physically. The effect of control changes at this point in time is small, with the consequence that a large control correction is needed in order to correct for a small error.

The region is characterized by large and erratic control corrections. The cross-check on the accuracy of the feedback gains (Section 3.4) indicates that the feedback data in this region are inaccurate. As explained in Section 3.4, large errors are encountered in inverting the near singular matrix $\underset{\sim}{Q}$. The cross check indicates that after a time of 160 days from the Earth, the error in some of the feedback gains is greater than 4%.

Since the state variations are approximately normal to the rows of the feedback gain matrix, an inaccuracy of 4% results in control corrections of which not even the sign is to be trusted. This problem was also encountered by Wood[4, 6] and Lattimore.[2]

A possible solution for this problem is to use nominal control. The question is now from what point in time should the nominal control only strategy be used. Or equivalently, what size of control changes can be tolerated without violating the linear assumptions. The cross-check on the feedback gain accuracy gives an indication of the time from which nominal control only should be used, but gives no specific value. This problem was circumvented by using nominal control from various times in the neighborhood of the predicted "switching time." The strategy used was then that one which gives the smallest terminal error. In Tables 1-8, the "best" switching time for each initial perturbation is given.

A second common problem is the time of termination of integration. The strategy used to overcome this problem is by defining a normalized norm of the terminal error,

$$E = \sum_{i=1}^{6} \frac{|x_i - x_{M_i}|}{|x_{M_i}|} ,$$

and continue integration until this norm starts to increase.

In all cases considered, the actual final time of the perturbed state, i.e., the integration termination time, was to within 0.5 days, the same as the first order predicted final time using the initial perturbation. Since the position and velocity of the vehicle matches the position and velocity of Mars closely (as will be seen from the results), the actual time of termination of the integration has very little effect on the terminal error, so that this problem is not very important.

Lattimore[2] used a minimum distance, closed loop guidance algorithm on the same transfer problem. He defined another problem area, namely the middle of the flight. It was found necessary to use nominal control during the middle of the flight. Since he does not define the "middle of the flight," it is unclear how this strategy was employed. In addition, the results indicate an error of $7.5959967022 \times 10^{-5}$ (AU) in position and an error of $7.5581577845 \times 10^{-3}$ AU/day in velocity for an initial perturbation in the x_1 velocity component of 5.0×10^{-6} AU/day. This means that the velocity error has grown by a factor of at least 1500 - a poor result if the performance of the guidance scheme is judged by the satisfaction of the terminal constraints only. A constant step size routine was used, and the use of nominal control during the "middle of the flight" was motivated by an argument that the perturbed control causes the time of the turn around period to shift slightly. This in turn causes large control corrections which exceed linearity so that the algorithm breaks down.

It is believed that this result is inaccurate. Certainly it is possible that a set of initial conditions can shift the time of turn around and that control changes will be larger in this region due to this fact, but for an initial perturbation of 5.0×10^{-6} AU/day the control changes calculated in this study did not exceed the limits of linearity. In implementing the algorithms presented in Chapter 4, it was not necessary to switch to nominal control during turn around.

Although the control changes are larger and again somewhat erratic during the middle 20% of the flight, it caused no trouble for any perturbations except the perturbation of 5.0×10^{-5} AU/day in the x_1 velocity component. Here it was found necessary to place an upper limit of 0.35 radians on the control change of u_2 and an upper limit of 0.15 radians on the control change of u_1. In addition, this upper limit was in effect only for two integration steps. It is believed that the fact that much smaller step sizes were employed during turn around in this study than in that of Lattimore contributes to the numerical stability experienced in this study during turn around. It is to be noted that the initial perturbation of 5.0×10^{-5} AU/day is ten times larger than the initial perturbation considered by Lattimore.

In addition, and/or alternatively, it is possible that inaccurate guidance information was generated by the scheme presented in Section 4.3 (maybe due to a programming error or very sensitive numerical behavior) and that this could be the reason for the poor satisfaction of the terminal constraint relations as found by Lattimore.[2]

Finally, it is to be noted that Hart and Lattimore carried all dependent variables in double precision in order to control roundoff. All computations in this study were done in single precision, since the errors introduced by single precision computation are much smaller than the truncation error introduced by numerical integration.

5.2 Results of the Flight Simulations

5.2.a Initial Perturbation in x_1 Velocity Component, Introduced at Zero Days

The set of initial perturbations in the x_1 velocity component range from -4.0×10^{-5} AU/day to $+5.0 \times 10^{-5}$ AU/day. The resulting Euclidian norms of the terminal velocity error and terminal position error are given in Figures 4 and 5, respectively.

For a velocity perturbation of -4.0×10^{-5} AU/day, the terminal velocity error is reduced by a factor of 4. For a velocity perturbation of -1.0 AU/day, the terminal velocity error is approximately the same as the initial error. There is hardly any difference between the performance of time-to-go and minimum distance.

For velocity perturbations greater than zero, time-to-go gives a slightly better terminal error than minimum distance, but the terminal error increases rapidly for perturbations larger than 2.0×10^{5} AU/day. Minimum distance guidance diverges for initial perturbations greater than 4.0×10^{5} AU/day.

To get a clear picture of the terminal position error, the initial perturbation should be put in a dimensionless form, since AU/day is not comparable with AU. The velocity variables can be put in dimensionless form by measuring the time in units of (the Earth's angular velocity about the sun)$^{-1}$, instead of in days.

Using this unit of time, the velocity perturbations AU/day must be multiplied by a factor

$$u = \frac{365.198084}{2\pi} \frac{\text{days}}{\text{year}} \Big/ \frac{\text{radians}}{\text{period}} .$$

Using this scale, it is seen that for a velocity perturbation in the range -2.0×10^{-5} to -4.0×10^{-5}, the terminal error is actually less than the initial error for both time-to-go and minimum distance guidance.

For perturbations between 1.8×10^{-5} and -1.0×10^{-5} AU/day, the terminal error is slightly greater than the initial error. Again there is hardly any difference between the performance of time-to-go versus minimum distance guidance.

As before, positive velocity perturbations less than 1.5×10^{-5} are handled slightly better by time-to-go guidance than by minimum distance guidance, and the reverse is true for initial velocity perturbations greater than 1.5×10^{-5}.

Tables 1 to 4 give the actual terminal error and the specific time from which nominal control only was used.

5.2.b <u>Initial Perturbation in x_4 Position Component, Introduced at Zero Days</u>

The set of initial perturbations in the x_4 position components ranges from -2.0×10^{-3} to -0.3×10^{-3} AU and from 0.3×10^{-3} to 3.3×10^{-3} AU. Note that a perturbation of 0.5×10^{-5} AU/day is comparable to a perturbation of 0.3×10^{-3} AU, so that the perturbations considered in part 5.2.a are comparable to those considered here.

As can be seen from Figure 6, minimum distance and time-to-go guidance exhibit approximately the same performance in minimizing the terminal error. The magnitude of the final error is slightly larger than the magnitude of the initial error for the smaller (in absolute value) perturbations, while the final error is smaller than the initial perturbation for larger initial perturbations.

Figure 7 must be interpreted with care. At points A and A^1 the terminal control strategy indicated that, by switching to the nominal control only strategy at a slightly different time, the terminal error can be reduced to 0.172×10^{-3} AU in the case of point A and to 0.192×10^{-3} AU in the case of point A^1. In the case of such a "conflicting" terminal control strategy, the strategy used was that which gives a minimum velocity error (see Figure 8).
For a rendezvous problem these errors are more significant than position errors. Observe that for all perturbations considered the terminal position errors are approximately ten times smaller than the initial perturbations.

In all the perturbations considered, this conflicting control strategy was encountered only with these two perturbations. The importance of the control strategy during the final stages of the flight is clearly illustrated by the above results.

Finally, it is to be noted that Lattimore considered an initial perturbation of 5.0×10^{-6} AU (approximately 60 times smaller than the smallest position perturbation considered in this study). The terminal velocity error for this perturbation was $6.8088261401 \times 10^{-3}$ AU/day. Putting this velocity error in a dimensionless form and dividing it by the initial perturbation (assuming that the magnitude of the perturbation considered is larger than any roundoff and turncation errors encountered during integration so that one should get a meaningful result), it is found that the error has increased by a factor of 78, 900. It is noted that this result is obtained by judging the guidance scheme by the satisfaction of the terminal constraints only. This is, however, the primary purpose of the guidance scheme, and the minimization of the transfer time is secondary.

A perturbation of such a small magnitude was not considered in this study, since it is smaller than the turncation errors encountered during the integration of the equations of motion. Any result from such a small error would be difficult to interpret.

In all cases considered, there is a "residual" terminal error. This error is due to roundoff and turncation errors encountered while integrating the non-linear equations of motion forward using a variational control history added to a nominal control history that was generated by backward integration. This error will always be present and is a result of the inherent inaccuracy of numerical integration.

5.2.c Initial Perturbation in x_3 Velocity and x_6 Position Components, Introduced at Zero Days

Results for out-of-plane perturbations are given in Figures 8 to 11 and in Tables 5 to 8.

The performance of time-to-go and minimum distance is again similar, except for perturbations less than -1.0×10^{-5} AU/day and -2.1×10^{-3} AU, where minimum distance guidance diverges very rapidly due to a poor estimate of the index time. In this region the linear assumptions 4.2.2 are invalid and an iterative procedure to evaluate the index time seems to be necessary.

Conclusions similar to that of paragraph 5.2 can be drawn.

5.3 A Second Minimum Distance Guidance Technique

A simulation with $k_0 = 0$, $k_i = 1$, $i = 1$ to 6 (see Equation 4.2.1) with initial perturbation 3.0×10^{-4} in x_4 was also run. The index time was calculated by Equations (4.2.3) and (4.2.4) summing i from 1 to 6. The velocity and position errors were found to be 0.6357898×10^{-5} AU/day and 0.1485626×10^{-3} AU, respectively. Comparing this with the results given in Figure 3, a slight improvement in the velocity error is sensed. The position error is unchanged.

5.4 Summary and Conclusions

It was shown in this study that, for the specific minimum distance metrics considered, there is no appreciable difference in the performance of the time-to-go and minimum distance techniques. In most cases, both techniques reduced the terminal error to a level lower than the initial error. In the cases where there are no reductions in the terminal error, this error was never greater than 2.5 times that of the initial error.

It was argued that, in general, the second order guidance schemes work well when compared to the performance of these schemes as found by Hart[1] and Lattimore.[2] When compared to the performance of the time-to-go guidance scheme as applied to a simplified version of the transfer problem, done by Wood,[4, 6] the time-to-go scheme is not as impressive. It is not possible to handle perturbations as large as those considered in this reference.

By minimizing different weighting functions of the form 4.2.1, better results can probably be obtained. This idea is illustrated for one isolated case.

The results stress the importance of the control strategy during the terminal stages of the flight. Since nominal control (which is non-optimal unless the vehicle is exactly on the nominal path) had to be used, there is not a large reduction in the initial error. It is possible that this period of non-optimal control conceals the relative merits of the guidance schemes, and for this reason it is unwise to come to any definite conclusion as to which works better.

A more rigorous technique for treating this period in the flight must be established. One possibility that might prove better than using nominal control is, for instance, to use open loop control for the last 20% of the flight.

Satisfaction of the terminal constraints can also be improved by taking more data points along the trajectory and doing matrix inversion in double precision. The accuracy of the terminal state appears to be limited by the accuracy of the feedback data at each point, the number of points, the various properties of the integration routine, and the specific control strategy used during the final stages of the flight.

It would be interesting to apply the minimum distance technique using (4.1.4) to compute the control change $d\underline{u}$ and an algorithm similar to the time-to-go algorithm employed in this study. It is believed that this method should yield better results.[14]

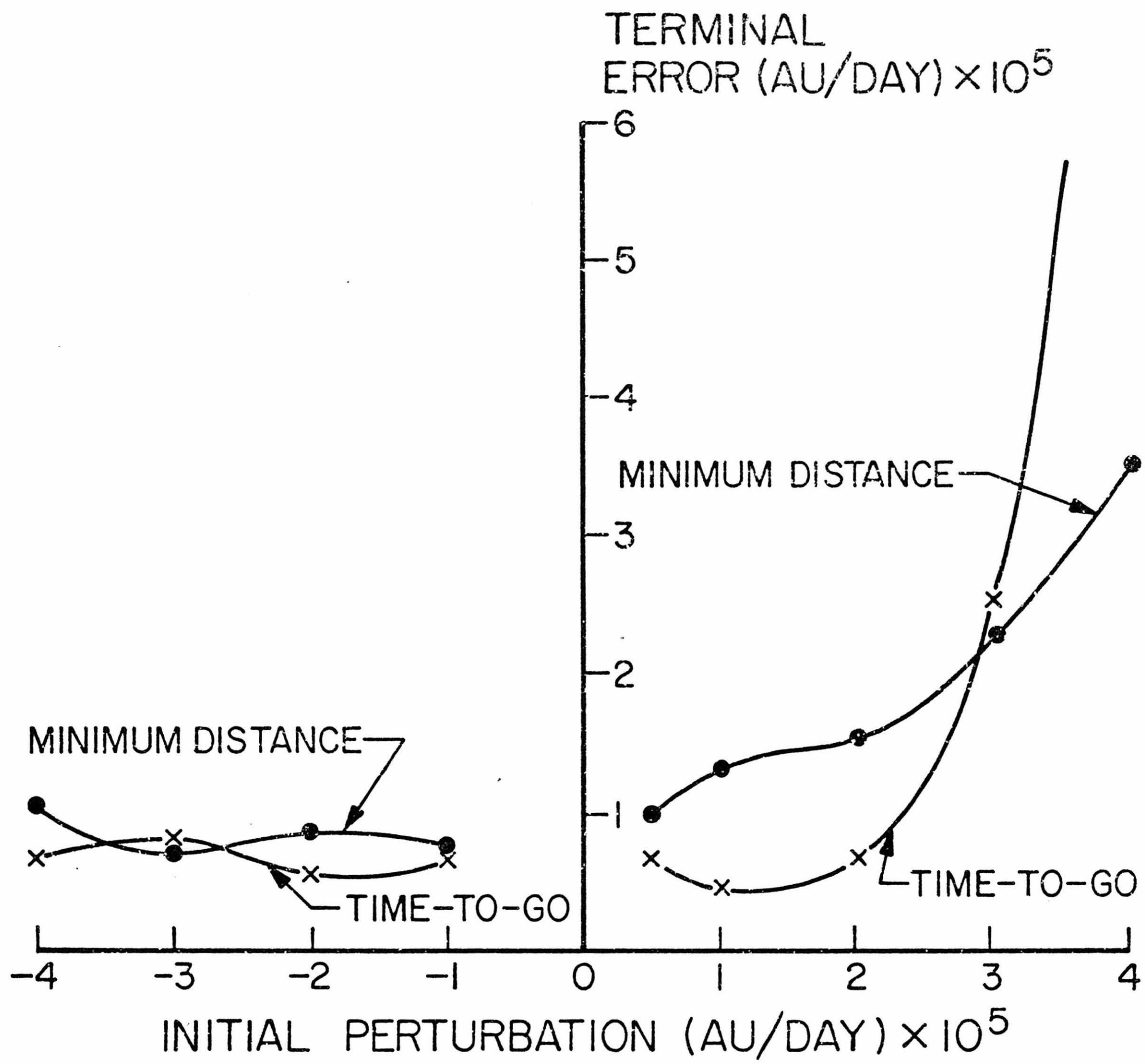

FIGURE 4

Terminal Velocity Error for an Initial Perturbation in x_1 Velocity, Introduced at Zero Days

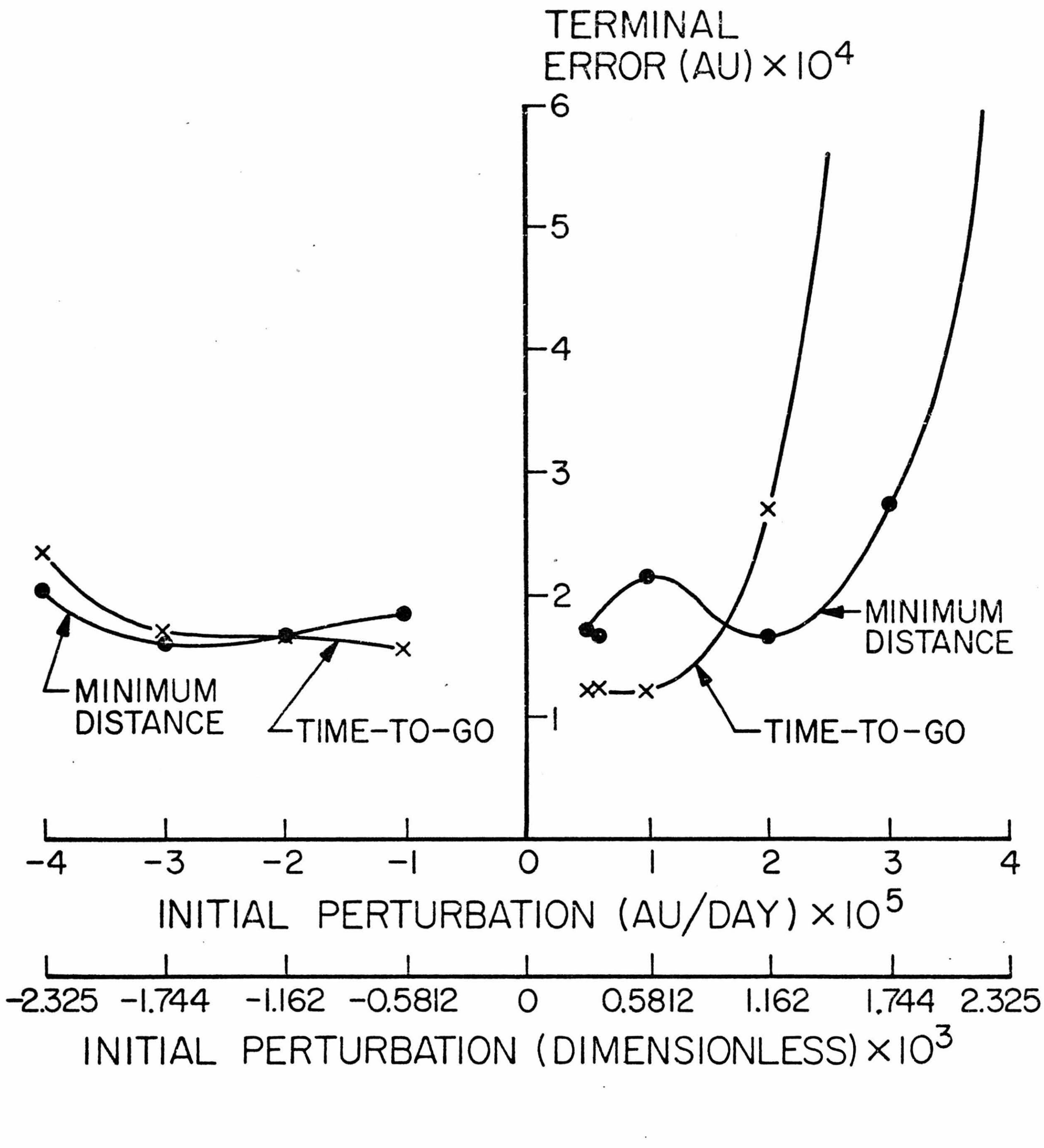

FIGURE 5

Terminal Position Error for an Initial Perturbation in x_1 Velocity, Introduced at Zero Days

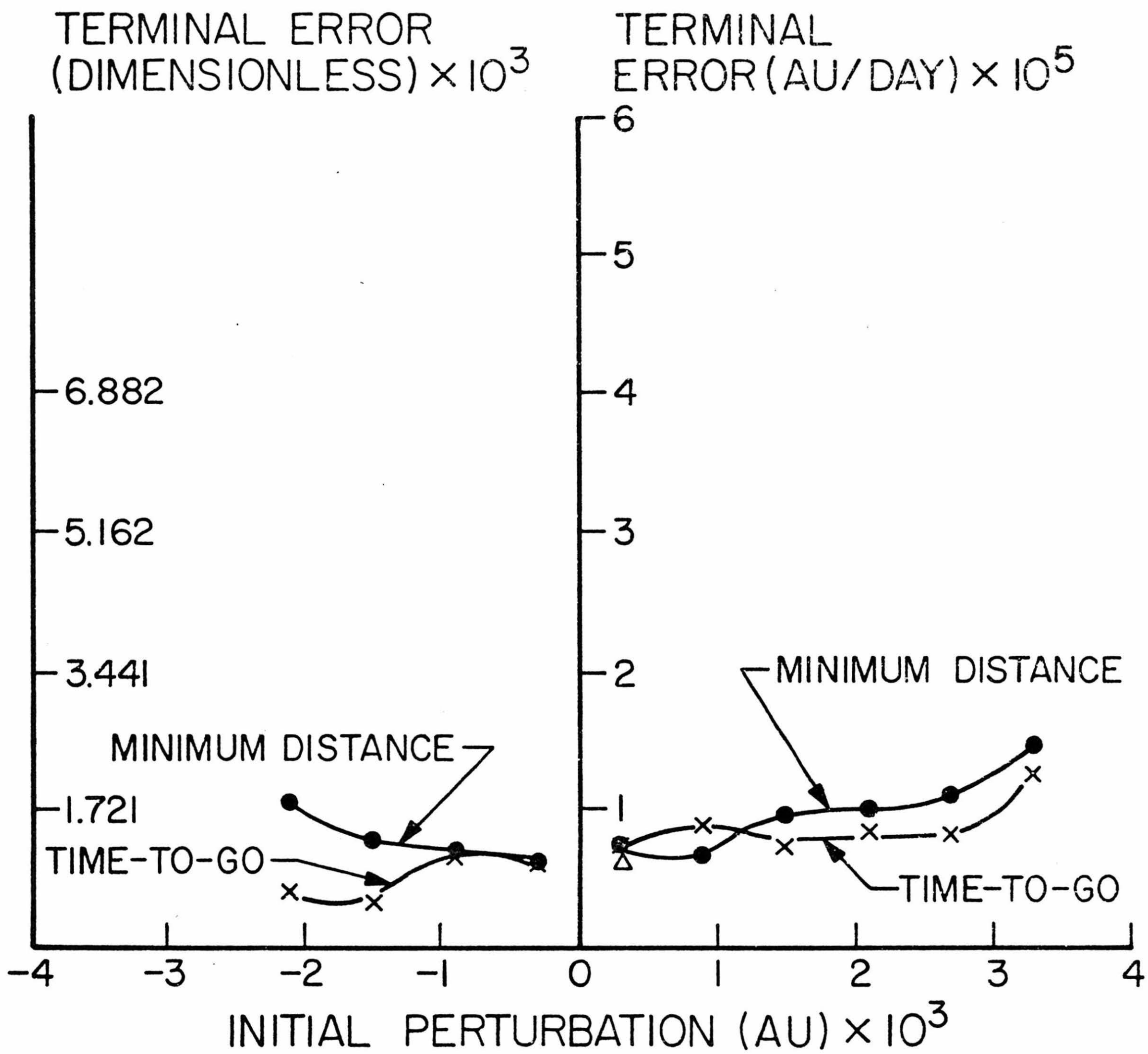

FIGURE 6

Terminal Velocity Error for an Initial Perturbation in x_4 Position, Introduced at Zero Days

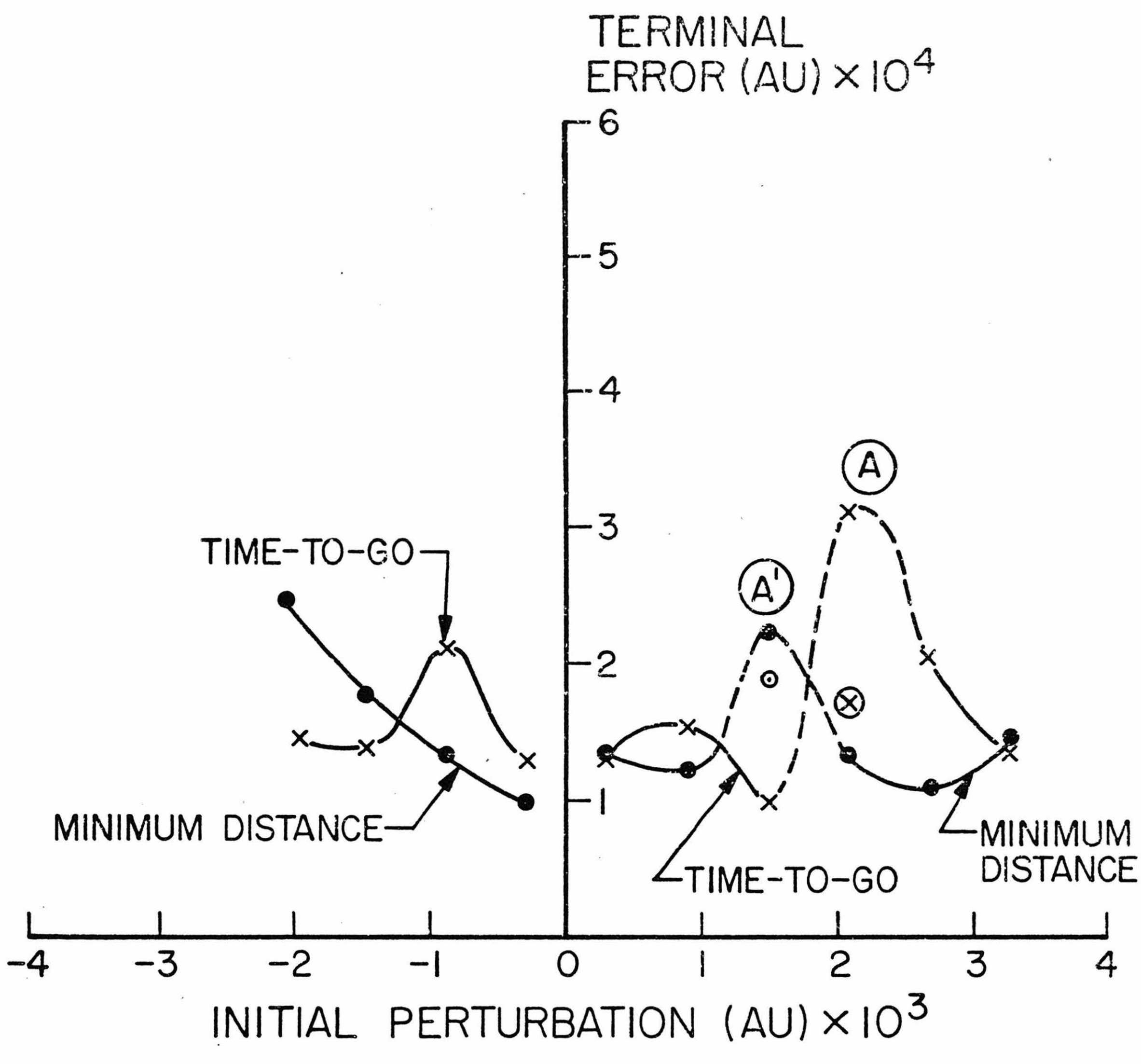

FIGURE 7

Terminal Position Error for an Initial Perturbation in x_4 Position, Introduced at Zero Days

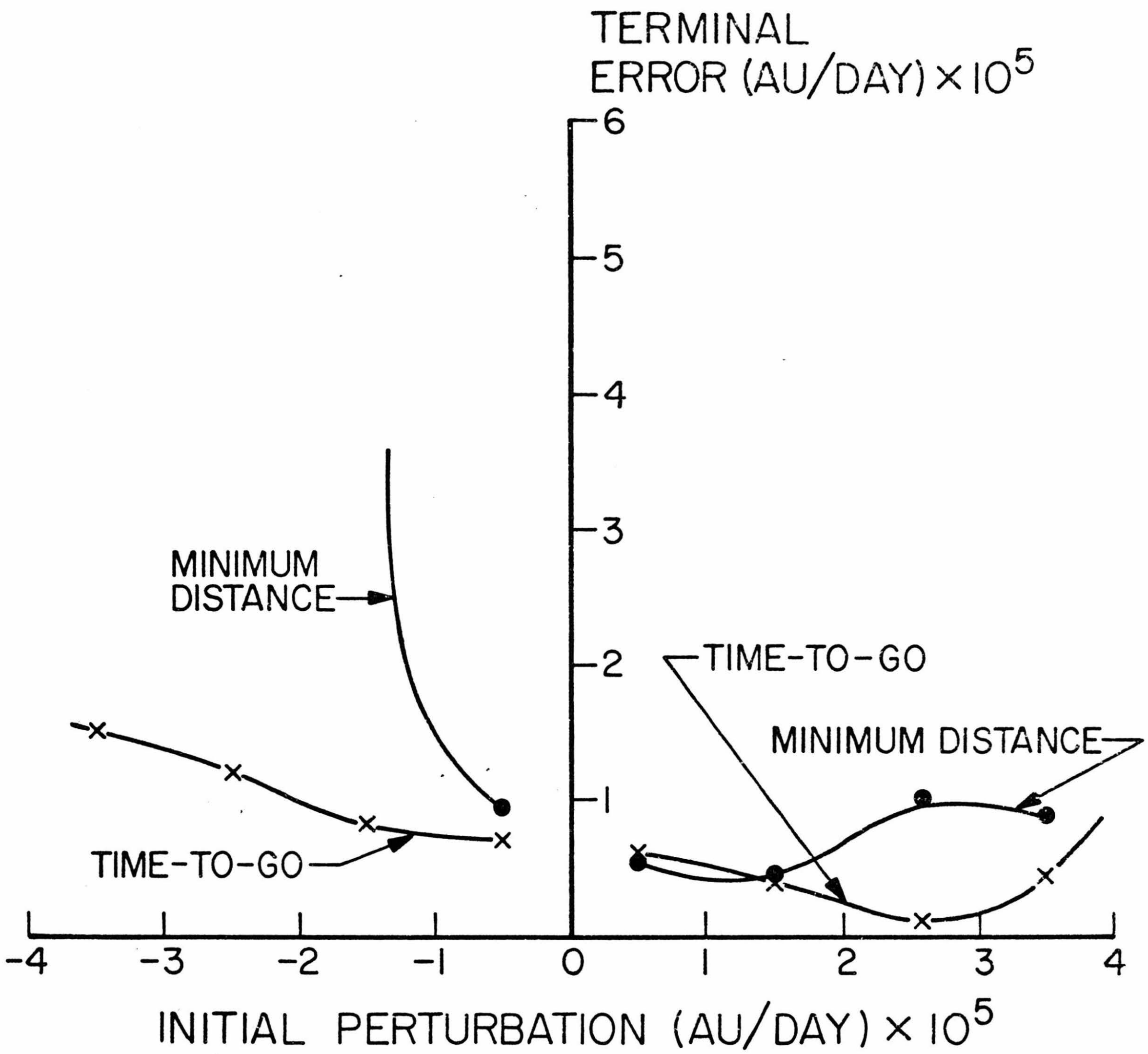

FIGURE 8

Terminal Velocity Error for an Initial Perturbation in x_3 Velocity, Introduced at Zero Days

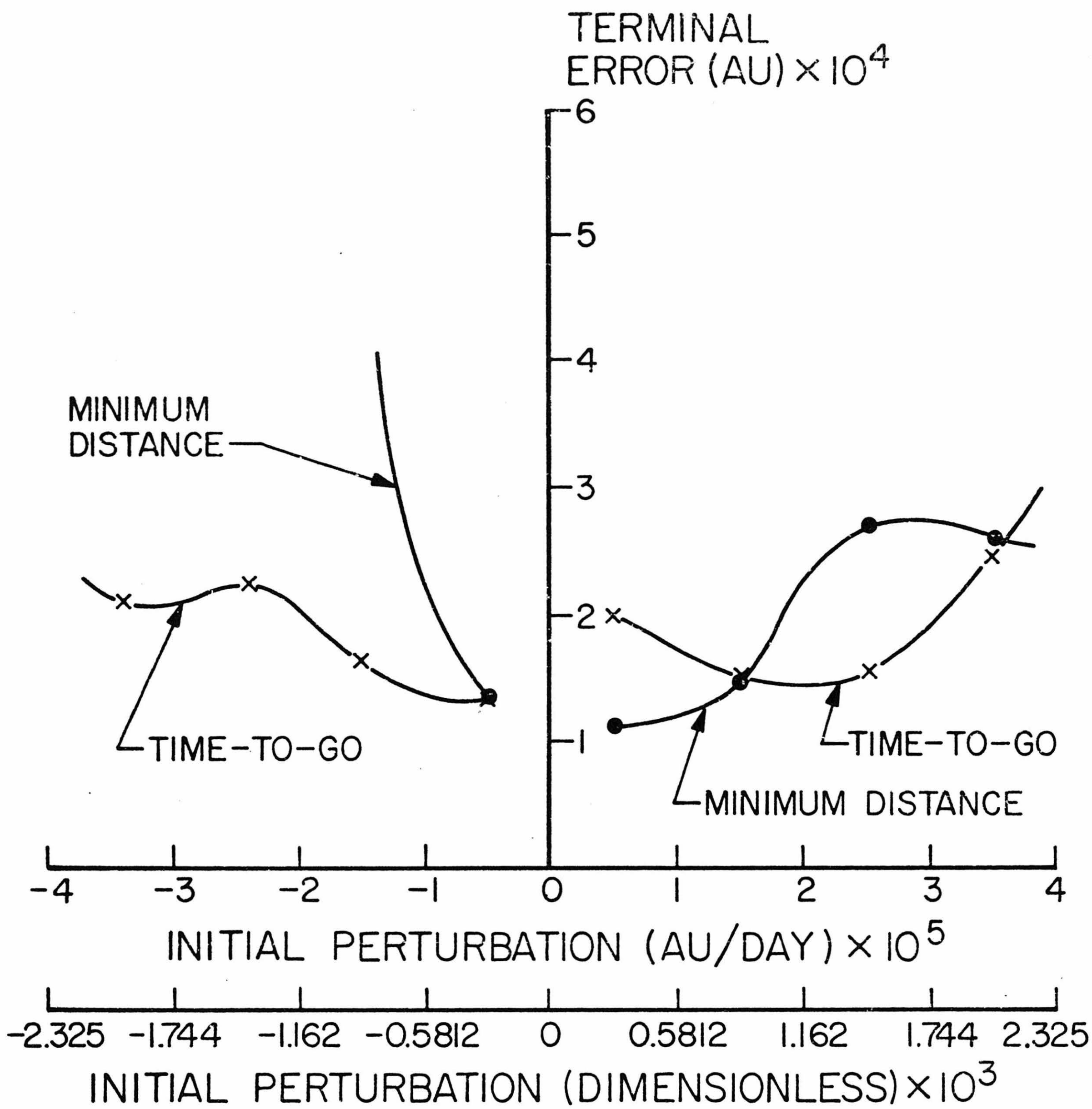

FIGURE 9

Terminal Position Error for an Initial Perturbation
in x_3 Velocity, Introduced at Zero Days

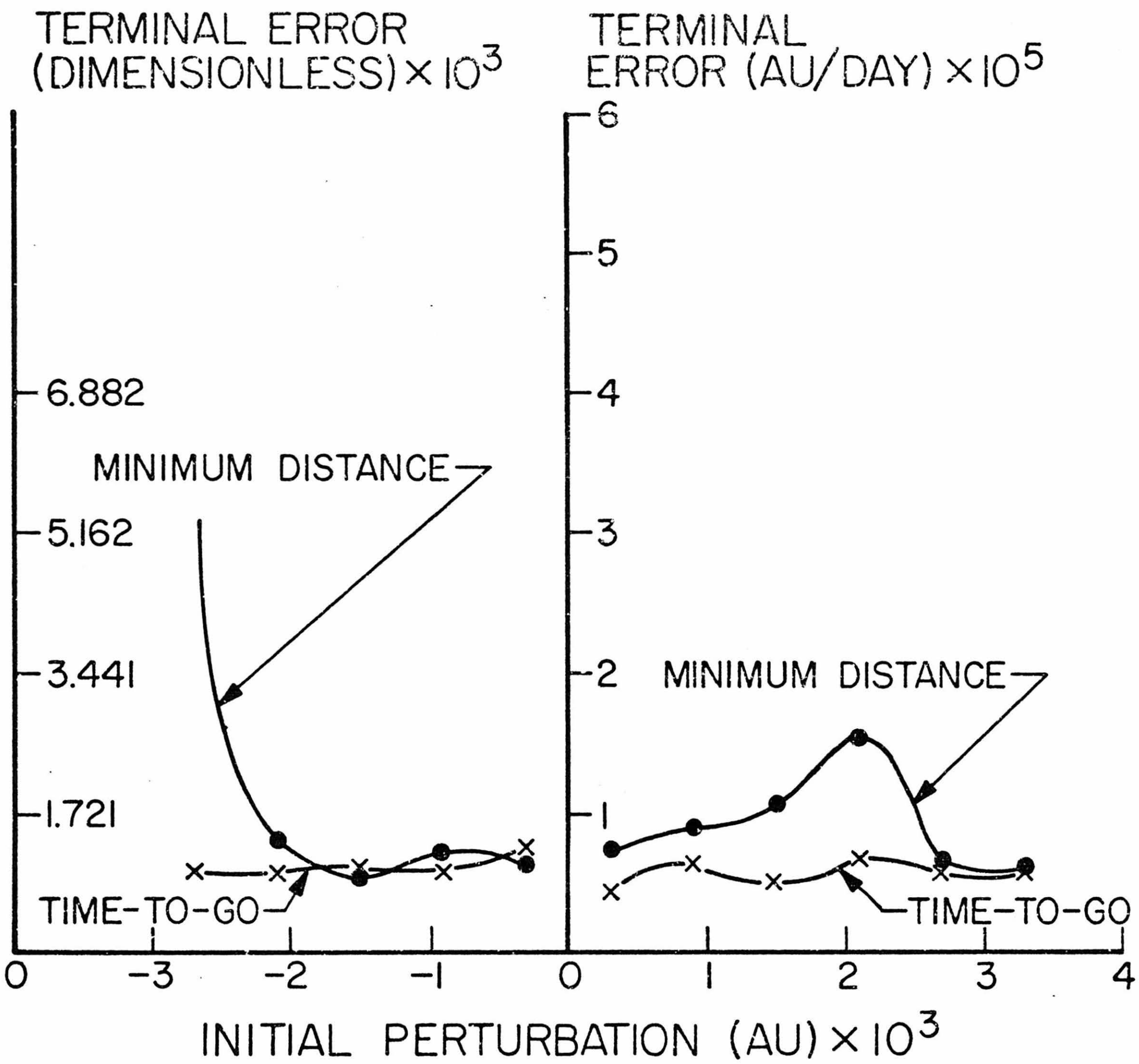

FIGURE 10

Terminal Velocity Error for an Initial Perturbation in x_6 Position, Introduced at Zero Days

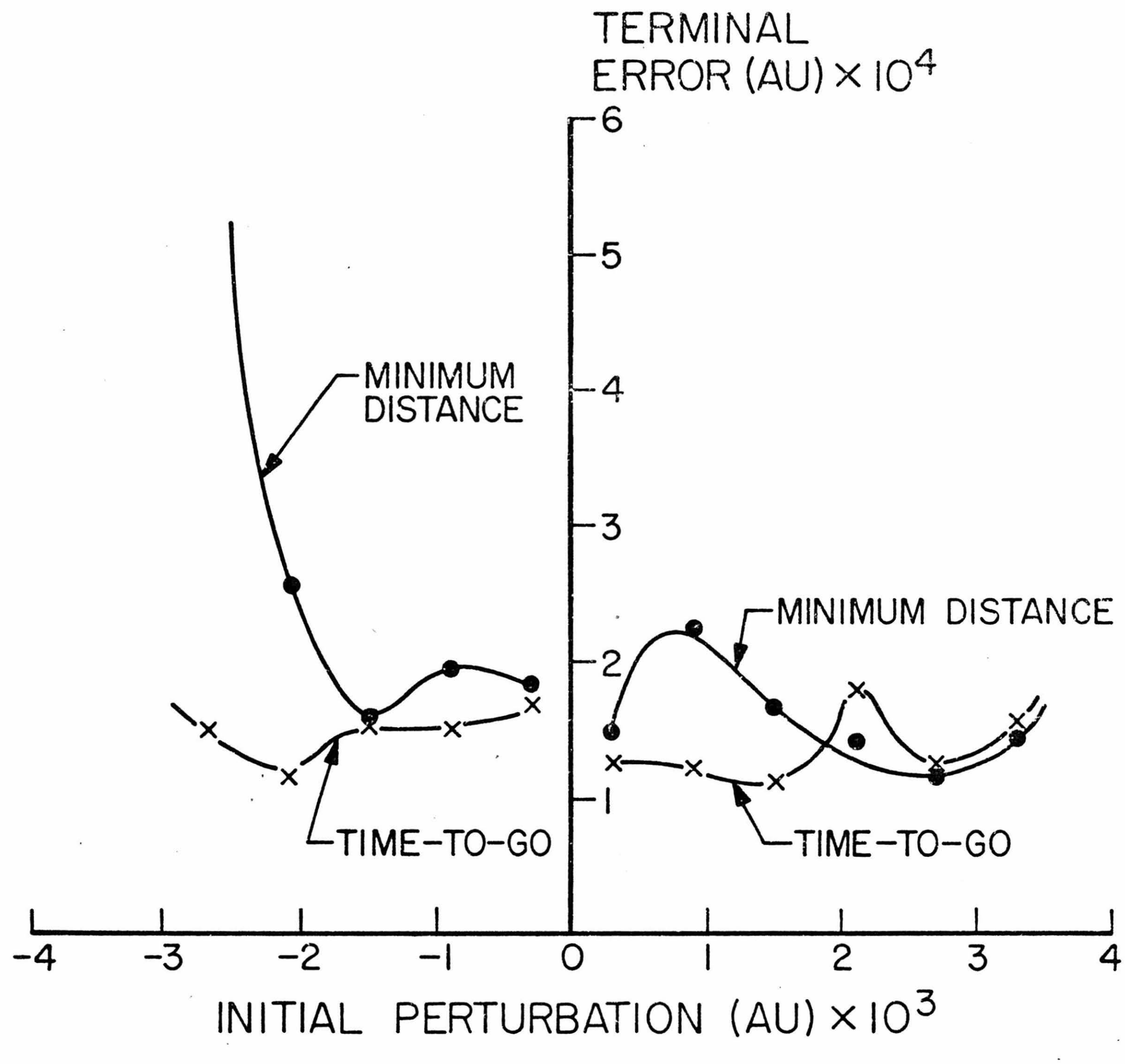

FIGURE 11

Terminal Position Error for an Initial Perturbation in x_6 Position, Introduced at Zero Days

TABLE 1

Terminal Error for an Initial Error in x_1 Velocity Component Introduced at Zero Days

Minimum Distance Guidance

δx_1 (AU/day)	$(x_1-x_{M_1})\times 10^5$	$(x_2-x_{M_2})\times 10^5$	$(x_3-x_{M_3})\times 10^5$	$(x_4-x_{M_4})\times 10^4$	$(x_5-x_{M_5})\times 10^4$	$(x_6-x_{M_6})\times 10^4$	T_{NC}*
-4×10^{-5}	0.6061047	-1.392141	0.4132744	0.0476837	-2.054572	-0.2995506	164.3072
-3×10^{-5}	-0.335648	-0.2540648	0.5668728	1.535416	-0.066162	0.467449	164.3072
-2×10^{-5}	0.1061708	-0.6120652	0.5900627	0.2479553	-1.607537	-0.1417100	166.0072
-1×10^{-5}	0.1300126	0.1806766	0.7253606	1.745224	0.3224611	0.5152076	166.0072
0.5×10^{-5}	-0.8210540	-0.2250075	0.5468028	0.0	-1.697540	-0.2472103	164.3072
1×10^{-5}	-1.193210	-0.0391156	0.5564652	-0.4482269	-2.435446	-0.5037338	166.0072
2×10^{-5}	-1.381338	0.5401671	0.4447764	0.8010864	-1.425743	-0.5469844	163.4572
3×10^{-5}	-1.108646	1.953542	0.4785368	2.307892	1.519322	0.1509860	163.4572
4×10^{-5}	-0.8970499	3.002957	1.5527240	6.551743	7.538199	3.357194	163.4572
5×10^{-5}	-0.3173947	6.268546	3.917119	10.27107	18.74149	12.58384	164.3072

*Time from which nominal control is used.

TABLE 2

Terminal Error for an Initial Error in x_1 Velocity Component, Introduced at Zero Days

Time-To-Go Guidance

δx_1 (AU/day)	$(x_1-x_{M_1})\times 10^5$	$(x_2-x_{M_2})\times 10^5$	$(x_3-x_{M_3})\times 10^5$	$(x_4-x_{M_4})\times 10^4$	$(x_5-x_{M_5})\times 10^4$	$(x_6-x_{M_6})\times 10^4$	T_{NC}*
-4×10^{-5}	0.1560897	0.5844980	0.2785819	2.822876	1.690984	0.7287785	164.3072
-3×10^{-5}	-0.2495944	-0.5956739	0.5515991	0.4959106	-1.635551	-0.1474842	164.3072
-2×10^{-5}	0.07413328	-0.2596527	0.4952075	1.497269	-0.1698732	0.2763420	164.3072
-1×10^{-5}	-0.2734363	-0.3505498	0.5121343	0.4291534	-1.401901	-0.287927	164.3072
0.5×10^{-5}	-0.06370246	-0.4228204	0.5413312	1.106262	-0.6526709	0.1418591	164.3072
1×10^{-5}	-0.07823110	-0.3516674	0.3272668	0.6580353	-0.9602308	-0.2980232	164.3072
2×10^{-5}	0.3859401	0.2309680	0.5069654	2.384186	1.301765	0.3450364	163.4572
3×10^{-5}	1.336634	2.065673	0.5489914	6.990433	7.901788	2.551191	163.4572
4×10^{-5}	10.24082	16.37340	6.350596	38.83362	65.35411	29.53283	163.4572
5×10^{-5}	20.84114	34.95999	20.05371	80.39474	155.9818	102.4807	163.4572

*Time from which nominal control is used.

TABLE 3

Terminal Error for an Initial Error in x_4 Position Component Introduced at Zero Days

Minimum Distance Guidance

δx_4 (AU)	$(x_1-x_{M1})\times10^5$	$(x_2-x_{M2})\times10^5$	$(x_3-x_{M3})\times10^5$	$(x_4-x_{M4})\times10^4$	$(x_5-x_{M5})\times10^4$	$(x_6-x_{M6})\times10^4$	T_{NC}*
-2.1×10^{-3}	-0.8095056	0.6012619	0.2899207	-0.2479553	-2.163649	-1.085326	163.4572
-1.5×10^{-3}	-0.6251037	0.3896654	0.3108988	0.4196167	-1.549721	-0.8240715	163.4572
-0.9×10^{-3}	-0.6001443	0.0145286	0.3730413	0.5435944	-1.227856	-0.3047287	164.3072
-0.3×10^{-3}	-0.3740191	0.0849366	0.4650792	0.7438660	-0.7224083	-0.0433996	166.0072
0.3×10^{-3}	-0.417605	-0.2734363	0.5111098	0.3433228	-1.354814	-0.0653788	166.0072
0.9×10^{-3}	-0.3416091	-0.3870577	0.453484	0.7247925	-1.004338	0.0397861	166.0072
1.5×10^{-3}	0.1322478	-0.1911074	0.8637784	1.897812	0.8058548	0.9533018	166.0072
2.1×10^{-3}	-0.1017004	-0.3609806	0.9267824	1.106262	-0.0268221	0.7338077	166.0072
2.7×10^{-3}	-0.0707805	-0.9808689	0.6636605	0.5054474	-0.9423494	0.3882870	166.0072
3.3×10^{-3}	-0.7808208	-0.8434057	0.8588424	1.077652	-0.3367662	0.9729713	166.0072

*Time from which nominal control is used.

TABLE 4

Terminal Error for an Initial Error in x_4 Position Component, Introduced at Zero Days

Time-To-Go Guidance

δx_4(AU)	$(x_1-x_{M_1})\times10^5$	$(x_2-x_{M_2})\times10^5$	$(x_3-x_{M_3})\times10^5$	$(x_4-x_{M_4})\times10^4$	$(x_5-x_{M_5})\times10^4$	$(x_6-x_{M_6})\times10^4$	T_{NC}*
-2.1×10^{-3}	0.3091991	0.2175570	0.1621655	1.373291	-0.1955032	-0.4678220	163.4572
-1.5×10^{-3}	0.0361353	-0.1654029	0.2670102	0.5912781	-1.130104	-0.6084144	163.4572
-0.9×10^{-3}	-0.2555549	-0.5360693	0.3310852	-0.0476837	-2.074838	-0.6743893	163.4572
-0.3×10^{-3}	0.024994	-0.2719462	0.5466165	1.125336	-0.6628036	0.8545816	166.0072
0.3×10^{-3}	-0.1028180	0.2305955	0.6759772	1.277924	0.2008677	0.3108382	166.0072
0.9×10^{-3}	-0.3524125	-0.7163733	0.4068948	0.1525879	-1.572967	-0.1869351	164.3072
1.5×10^{-3}	-0.0853092	-0.3974885	0.6413320	0.8869171	-0.4619360	0.3332645	166.0072
2.1×10^{-3}	-0.1452863	0.0752509	0.8357922	2.489090	1.621246	1.208745	166.0072
2.7×10^{-3}	-0.0048429	-0.3322959	0.7380499	1.802444	0.6574392	0.8461997	166.0072
3.3×10^{-3}	-0.3218651	-0.6046146	1.061661	1.077652	-0.0780821	0.8646771	166.0072

*Time from which nominal control is used.

TABLE 5

Terminal Error for an Initial Error in x_3 Velocity Component, Introduced at Zero Days

Minimum Distance Guidance

δx_3 (AU/day)	$(x_1-x_{M_1})\times10^5$	$(x_2-x_{M_2})\times10^5$	$(x_3-x_{M_3})\times10^5$	$(x_4-x_{M_4})\times10^4$	$(x_5-x_{M_5})\times10^4$	$(x_6-x_{M_6})\times10^4$	T_{NC}*
-1.5×10^{-5}	5.701184	26.00774	30.59092	-1.096725	79.23126	177.1349	163.4572
-0.5×10^{-5}	-0.1106411	0.3412366	0.9254320	1.192093	-0.1388788	0.6292388	166.0072
0.5×10^{-5}	-0.4246831	-0.1687557	0.3842171	0.7343292	-0.8755922	-0.1218170	166.0072
1.5×10^{-5}	-0.3777444	-0.1862645	0.2417713	0.5817413	-1.145005	-0.7681549	164.3072
2.5×10^{-5}	-0.8482486	0.5669892	-0.1622364	-0.1621246	-1.970530	-1.874231	164.3072
3.5×10^{-5}	-0.6407499	0.6340444	-0.0725035	0.6294250	-0.9232759	-1.677759	164.3072

*T_{NC} = time from which nominal control is used.

TABLE 6

Terminal Error for an Initial Error in x_6 Position Component, Introduced at Zero Days

Minimum Distance Guidance

δx_6(AU)	$(x_1-x_{M_1})\times10^5$	$(x_2-x_{M_2})\times10^5$	$(x_3-x_{M_3})\times10^5$	$(x_4-x_{M_4})\times10^4$	$(x_5-x_{M_5})\times10^4$	$(x_6-x_{M_6})\times10^4$	T_{NC}*
-2.7×10^{-3}	19.28583	34.6303	19.37522	69.54193	141.2106	95.85414	164.3072
-2.1×10^{-3}	-0.6645918	-0.3755093	0.3144844	-0.4100800	-2.474785	-0.5971640	166.0072
-1.5×10^{-3}	-0.4697591	-0.1542270	0.2811663	0.2574921	-1.521707	-0.3860518	164.3072
-0.9×10^{-3}	-0.058471	0.3200024	0.6527407	1.773834	0.6145239	0.5266443	166.0072
-0.3×10^{-3}	-0.4623085	-0.1527369	0.4298054	0.1430511	-1.786351	-0.4812703	164.3072
0.3×10^{-3}	-0.1024455	-0.2346933	0.6925547	1.430511	1.215935	0.3879145	166.0072
0.9×10^{-3}	-0.8512288	0.3229827	0.1198612	-0.1430511	-2.021194	-1.085922	164.3072
1.5×10^{-3}	-0.8814037	0.6094575	0.2513174	0.4482269	-1.371503	-0.9364394	163.4572
2.1×10^{-3}	-0.5763024	1.392141	0.3484543	0.9059906	-0.4959106	-1.069382	163.4572
2.7×10^{-3}	-0.3043562	0.064820	0.5732290	0.6294250	-0.9691715	-0.034624	166.0072
3.3×10^{-3}	-0.3438443	0.0610947	0.5324604	0.5054474	-1.338124	-0.2681091	166.0072

*T_{NC} = time from which nominal control is used.

TABLE 7

Terminal Error of an Initial Error in x_3 Velocity Component, Introduced at Zero Days

Time-To-Go Guidance

δx_3 (AU/day)	$(x_1-x_{M_1})\times10^5$	$(x_2-x_{M_2})\times10^5$	$(x_3-x_{M_3})\times10^5$	$(x_4-x_{M_4})\times10^4$	$(x_5-x_{M_5})\times10^4$	$(x_6-x_{M_6})\times10^4$	T_{NC}*
-3.5×10^{-5}	0.1426786	-0.1810491	1.421990	1.316071	-0.4869699	1.573116	166.0072
-2.5×10^{-5}	-0.2846122	-0.6794930	1.000962	0.0286102	-2.146363	0.6939843	164.3072
-1.5×10^{-5}	0.0242144	-0.3039837	0.8230098	1.382828	-0.2652407	0.8341670	166.0072
-0.5×10^{-5}	-0.0558794	-0.359026	0.6953487	0.6103516	-1.205802	0.05591661	164.3072
0.5×10^{-5}	0.3594905	0.2354383	0.5182810	1.821518	0.9554625	0.3174320	166.0072
1.5×10^{-5}	-0.1933426	-0.3524125	0.1316890	0.4196167	-1.187921	-0.9078160	164.3072
2.5×10^{-5}	0.1505017	-0.0007451	0.0755768	1.420975	0.8225441	-0.6349385	166.0072
3.5×10^{-5}	0.3594905	0.3028661	-0.0960426	2.031326	1.275539	-0.6538257	166.0072

*T_{NC} = time from which nominal control is used.

TABLE 8

Terminal Error for an Initial Error in x_6 Position Component, Introduced at Zero Days

Time-To-Go Guidance

δx_6 (AU)	$(x_1-x_{M_1})\times10^5$	$(x_2-x_{M_2})\times10^5$	$(x_3-x_{M_3})\times10^5$	$(x_4-x_{M_4})\times10^4$	$(x_5-x_{M_5})\times10^4$	$(x_6-x_{M_6})\times10^4$	T_{NC}*
-2.7×10^{-3}	-0.1292676	-0.4712492	0.3733207	0.7438660	-1.302361	-0.1228973	164.3072
-2.1×10^{-3}	-0.2440065	-0.3736466	0.3995374	0.8678436	-0.7897615	0.0924989	164.3072
-1.5×10^{-3}	-0.1333654	-0.451502	0.4203524	0.6866455	-1.339912	-0.211820	164.3072
-0.9×10^{-3}	-0.1158565	-0.3855675	0.4365807	0.4386902	-1.407862	-0.2951920	164.3072
-0.3×10^{-3}	0.3360212	0.2305955	0.6525312	1.649857	0.6377697	0.3818050	166.0072
0.3×10^{-3}	-0.1106411	-0.1996756	0.4202127	1.277924	-0.1651049	0.1794472	164.3072
0.9×10^{-3}	-0.0655651	-0.3706664	0.5640788	0.6675720	-1.029968	-0.0228360	166.0072
1.5×10^{-3}	-0.0450760	-0.2644956	0.4440080	0.8773804	-0.6937981	-0.0408292	166.0072
2.1×10^{-3}	-0.2089888	-0.531989	0.4251255	0.3337860	-1.738667	-0.4559010	164.3072
2.7×10^{-3}	0.1233071	-0.0842673	0.5766517	1.249313	-0.3290176	0.1177937	166.0072
3.3×10^{-3}	-0.1307182	-0.4243106	0.3870344	0.4386902	-1.478195	-0.4903600	164.3072

*T_{NC} = Time from which nominal control is used.

APPENDIX 1

1.1 Earth Orbital Data

Semi-major axis, a_E	1.0 AU
Eccentricity, e_E	0.016726
Argument of perihelion, ω_E	0.0°
Angle of inclination, i_E	0.0°
Argument of ascending node, Ω_E	0.0°
Time of perihelion	Jan. 3.022307069, 1950
Period	365.198084 days

1.2 Mars Orbital Data

Semi-major axis, a_M	1.523691 AU
Eccentricity, e_M	0.093393
Argument of perihelion, ω_M	286.07366°
Angle of inclination, i_M	1.84991°
Argument of ascending node, Ω_M	0.0°
Time of perihelion	March 17.490627, 1950
Period	686.868886 days

1.3 Vehicle- and other constants

Mass flow rate, β	0.00108 (initial vehicle mass/day)
Exhaust speed, C	0.045365 AU/day
Initial spacecraft mass, m_0	1.0
Solar gravitational constant, μ	$2.96007536 \times 10^{-4}$ AU^3/day^2

APPENDIX 2

The initial conditions for the set of differential Equations (2.2.1) and (2.3.4b) are:

$$x_1 = -1.4835073 \times 10^{-2}$$

$$x_2 = 9.2714508 \times 10^{-3}$$

$$x_3 = 0.0$$

$$x_4 = 5.199345 \times 10^{-1}$$

$$x_5 = 8.3463802 \times 10^{-1}$$

$$x_6 = 0.0$$

$$\lambda_1 = 1.006871 \times 10^{1}$$

$$\lambda_2 = -2.135045 \times 10^{1}$$

$$\lambda_3 = -6.701413 \times 10^{-1}$$

$$\lambda_4 = -5.168126 \times 10^{-2}$$

$$\lambda_5 = -4.327681 \times 10^{-1}$$

$$\lambda_6 = -1.323293 \times 10^{-3}$$

APPENDIX 3

The objective of this appendix is to summarize all the equations used in this study. For clarity, a brief indication of how they were derived will be given.

A1 The Differential Equations of Motion

The non-linear set of ordinary differential equations of motion are

$$\dot{x}_1 = -\mu \frac{x_4}{r^3} + \frac{T}{m} \cos u_1 \cos u_2$$

$$\dot{x}_2 = -\mu \frac{x_5}{r^3} + \frac{T}{m} \cos u_1 \sin u_2$$

$$\dot{x}_3 = -\mu \frac{x_6}{r^3} + \frac{T}{m} \sin u_1 \qquad \text{(A. 1. 1)}$$

$$\dot{x}_4 = x_1$$

$$\dot{x}_5 = x_2$$

$$\dot{x}_6 = x_3$$

A2 The Performance Index, Hamiltonian, and First Order Necessary Conditions

The performance index for minimizing transfer time can be written as

$$J = \int_{t_o}^{t_f} \beta \cdot dt \, . \qquad \text{(A. 2. 1)}$$

The Hamiltonian, defined as $H = L + \underline{\lambda}^T \underline{f}$, then becomes

$$H = 1 + \lambda_1\left(-\mu \frac{x_4}{r^3} + \frac{T}{m} \cos u_1 \cos u_2\right) + \lambda_2\left(-\mu \frac{x_5}{r^3} + \frac{T}{m} \cos u_1 \sin u_2\right)$$

$$+ \lambda_3\left(-\mu \frac{x_6}{r^3} + \frac{T}{m} \sin u_1\right) + \lambda_4 x_1 + \lambda_5 x_2 + \lambda_6 x_3 \ . \qquad \text{(A.2.2)}$$

The first order necessary conditions (2.3.4b) and (2.3.4c) yield

$$\dot{\lambda}_1 = -\lambda_4$$

$$\dot{\lambda}_2 = -\lambda_5$$

$$\dot{\lambda}_3 = -\lambda_6$$

$$\dot{\lambda}_4 = \frac{\mu\lambda_1}{r^3} - \frac{3\mu x_4}{r^5}(\lambda_1 x_4 + \lambda_2 x_5 + \lambda_3 x_6) \qquad \text{(A.2.3)}$$

$$\dot{\lambda}_5 = \frac{\mu\lambda_2}{r^3} - \frac{3\mu x_5}{r^5}(\lambda_1 x_4 + \lambda_2 x_5 + \lambda_3 x_6)$$

$$\dot{\lambda}_6 = \frac{\mu\lambda_3}{r^3} - \frac{3\mu x_6}{r^5}(\lambda_1 x_4 + \lambda_2 x_5 + \lambda_3 x_6)$$

$$\lambda_1 \sin u_1 \cos u_2 + \lambda_2 \sin u_1 \sin u_2 - \lambda_3 = 0 \qquad \text{(A.2.4)}$$

$$\lambda_1 \cos u_1 \sin u_2 + \lambda_2 \cos u_1 \cos u_2 = 0$$

Using the fact that for a minimum we must have $H_{\underline{u}\,\underline{u}} > 0$, Equations (A.2.4) can be solved for u_1, u_2. Thus,

$$\sin u_1 = \frac{-\lambda_3}{\sqrt{\lambda_1^2 + \lambda_2^2 + \lambda_3^2}}$$

$$\cos u_1 = \frac{\sqrt{\lambda_1^2 + \lambda_2^2}}{\sqrt{\lambda_1^2 + \lambda_2^2 + \lambda_3^2}}$$

$$\sin u_2 = \frac{-\lambda_2}{\sqrt{\lambda_1^2 + \lambda_2^2}} \qquad \text{(A. 2. 5)}$$

$$\cos u_2 = \frac{-\lambda_1}{\sqrt{\lambda_1^2 + \lambda_2^2}}$$

A3 The Second Variation

A3.i The Matrices $H_{\underline{u}\,\underline{u}}^{-1}$, $H_{\underline{x}\,\underline{x}}$, $H_{\underline{u}\,\underline{x}}$, $H_{\underline{x}\,\underline{u}}$

These matrices are easily calculated using Equation (A. 2. 2). They are

$$H_{\underline{u}\,\underline{u}}^{-1} = \begin{bmatrix} \dfrac{1}{\frac{T}{m}\sqrt{\lambda_1^2 + \lambda_2^2 + \lambda_3^2}} & 0 \\ 0 & \dfrac{\sqrt{\lambda_1^2 + \lambda_2^2 + \lambda_3^2}}{\frac{T}{m}(\lambda_1^2 + \lambda_2^2)} \end{bmatrix} \qquad \text{(A. 3. 1)}$$

$$H_{\underline{x}\,\underline{x}} = \begin{bmatrix} \underset{3\times 3}{0} & \underset{3\times 3}{0} \\ \underset{3\times 3}{0} & \begin{matrix} H_{x_4x_4} & H_{x_5x_4} & H_{x_6x_4} \\ H_{x_4x_5} & H_{x_5x_5} & H_{x_6x_5} \\ H_{x_4x_6} & H_{x_5x_6} & H_{x_6x_6} \end{matrix} \end{bmatrix} \qquad \text{(A. 3. 2)}$$

where

$$H_{x_4x_4} = \frac{3\mu}{r^5}(3\lambda_1 x_4 + \lambda_2 x_5 + \lambda_3 x_6) - \frac{15\mu}{r^7} x_4^2(\lambda_1 x_4 + \lambda_2 x_5 + \lambda_3 x_6)$$

$$H_{x_5x_5} = \frac{3\mu}{r^5}(\lambda_1 x_4 + 3\lambda_2 x_5 + \lambda_3 x_6) - \frac{15\mu}{r^7} x_5^2(\lambda_1 x_4 + \lambda_2 x_5 + \lambda_3 x_6)$$

$$H_{x_6x_6} = \frac{3\mu}{r^5}(\lambda_1 x_4 + \lambda_2 x_5 + 3\lambda_3 x_6) - \frac{15\mu}{r^7} x_6^2(\lambda_1 x_4 + \lambda_2 x_5 + \lambda_3 x_6)$$

$$H_{x_4x_5} = \frac{3\mu}{r^5}(\lambda_1 x_5 + \lambda_2 x_4) - \frac{15\mu}{r^7} x_4 x_5(\lambda_1 x_4 + \lambda_2 x_5 + \lambda_3 x_6)$$

$$H_{x_4x_6} = \frac{3\mu}{r^5}(\lambda_1 x_6 + \lambda_3 x_4) - \frac{15\mu}{r^7} x_4 x_6(\lambda_1 x_4 + \lambda_2 x_5 + \lambda_3 x_6)$$

$$H_{x_5x_6} = \frac{3\mu}{r^5}(\lambda_2 x_6 + \lambda_3 x_5) - \frac{15\mu}{r^7} x_5 x_6(\lambda_1 x_4 + \lambda_2 x_5 + \lambda_3 x_6)$$

$$H_{ux} = \underset{2\times 6}{0} \qquad \text{(A. 3. 3)}$$

$$H_{xu} = \underset{6\times 2}{0} \qquad \text{(A. 3. 4)}$$

A3. ii The Matrices $\underline{f}_{\underline{x}}, \underline{f}_{\underline{u}}$

Noting that $\dot{\underline{x}} = \underline{f}(\underline{x}, \underline{u}, t)$, $\underline{f}_{\underline{x}}$ and $\underline{f}_{\underline{u}}$ are calculated from A. 1. 1

$$\underline{f}_{\underline{x}} = \begin{bmatrix} \underset{3\times 3}{0} & \begin{matrix} \frac{3\mu x_4^2}{r^5} - \frac{\mu}{r^3} & \frac{3\mu x_4 x_5}{r^5} & \frac{3\mu x_4 x_6}{r^5} \\ \frac{3\mu x_4 x_5}{r^5} & \frac{3\mu x_5^2}{r^5} - \frac{\mu}{r^3} & \frac{3\mu x_5 x_6}{r^5} \\ \frac{3\mu x_4 x_6}{r^5} & \frac{3\mu x_5 x_6}{r^5} & \frac{3\mu x_6^2}{r^5} - \frac{\mu}{r^3} \end{matrix} \\ \underset{3\times 3}{I} & \underset{3\times 3}{0} \end{bmatrix} \tag{A.3.5}$$

$$\underline{f}_{\underline{u}} = \frac{T}{m} \begin{bmatrix} -\sin u_1 \cos u_2 & -\cos u_1 \sin u_2 \\ -\sin u_1 \sin u_2 & \cos u_1 \cos u_2 \\ \cos u_1 & 0 \\ 0 & 0 \\ 0 & 0 \\ 0 & 0 \end{bmatrix} \tag{A.3.6}$$

A3.iii Calculation of A(t), B(t), C(t)

Using (2.3.11) - (2.3.13) together with (A.3.1) - (A.3.4) and the above

$$\begin{aligned} A(t) &= \underline{f}_{\underline{x}} \\ B(t) &= \underline{f}_{\underline{u}} H_{\underline{u}\underline{u}}^{-1} \underline{f}_{\underline{u}}^{T} \\ C(t) &= H_{\underline{x}\underline{x}} \end{aligned} \tag{A.3.7}$$

A4 Boundary Conditions for the Differential Equations (2.3.18)

A4.i The Terminal Constraint Relations

Since a rendezvous problem is considered, there are six terminal constraint relations

$$\underline{Y}(\underline{x}_f, t_f) = \underline{x}(t_f) - \underline{x}_M(t_f) = \underline{0} \qquad \text{(A. 4. 1)}$$

where

$$x_{M_1}(t_f) = -a_M\dot{E}_f\{\cos \omega_M \sin E_f + (1 - e_M^2)^{\frac{1}{2}} \sin \omega_M \cos E_f\}$$

$$x_{M_2}(t_f) = a_M\dot{E}_f \cos i_M\{-\sin \omega_M \sin E_f + (1 - e_M^2)^{\frac{1}{2}} \cos \omega_M \cos E_f\}$$

$$x_{M_3}(t_f) = a_M\dot{E}_f \sin i_M\{-\sin \omega_M \sin E_f + (1 - e_M^2)^{\frac{1}{2}} \cos \omega_M \cos E_f\}$$

$$\text{(A. 4. 2)}$$

$$x_{M_4}(t_f) = a_M\{\cos \omega_M(\cos E_f - e_M) - (1 - e_M^2)^{\frac{1}{2}} \sin \omega_M \sin E_f\}$$

$$x_{M_5}(t_f) = a_M \cos i_M\{\sin \omega_M(\cos E_f - e_M) + (1 - e_M^2)^{\frac{1}{2}} \cos \omega_M \sin E_f\}$$

$$x_{M_6}(t_f) = a_M \sin i_M\{\sin \omega_M(\cos E_f - e_M) + (1 - e_M^2)^{\frac{1}{2}} \cos \omega_M \sin E_f\} .$$

E_f is the eccentric anomaly of Mars at t_f and it satisfies Keplers equation:

$$E_f - e_M \sin E_f = t_f\left(\frac{\mu}{a_M^3}\right)^{\frac{1}{2}} + E_0 - e_M \sin E_0 , \qquad \text{(A. 4. 3)}$$

where $E_0 = 178.995341°$ is the eccentric anomaly of Mars at t_0. Differentiating A. 4. 2 and A. 4. 3 with respect to time, we find

$$\dot{x}_{M_1}(t_f) = -a_M\ddot{E}_f\{\cos \omega_M \sin E_f + (1 - e_M^2)^{\frac{1}{2}} \sin \omega_M \cos E_f\} -$$

$$a_M\dot{E}_f^2\{\cos \omega_M \cos E_f - (1 - e_M^2)^{\frac{1}{2}} \sin \omega_M \sin E_f\} ,$$

$$\ddot{x}_{M_1}(t_f) = a_M(\dot{E}_f^{\,3} - \dddot{E}_f)\{\cos\omega_M \sin E_f + (1 - e_M)^{\frac{1}{2}} \sin\omega_M \cos E_f\}$$

$$-3a_M \ddot{E}_f \dot{E}_f\{\cos\omega_M \cos E_f - (1 - e_M)^{\frac{1}{2}} \sin\omega_M \sin E_f\} ,$$

$$\dot{x}_{M_2}(t_f) = a_M \ddot{E}_f \cos i_M\{-\sin\omega_M \sin E_f + (1 - e_M)^{\frac{1}{2}} \cos\omega_M \cos E_f\} -$$

$$a_M \dot{E}_f^{\,2} \cos i_M\{\sin\omega_M \cos E_f + (1 - e_M)^{\frac{1}{2}} \cos\omega_M \sin E_f\} ,$$

$$\ddot{x}_2(t_f) = a_M \cos i_M[(\dddot{E}_f - \dot{E}_f^{\,3})\{-\sin\omega_M \sin E_f + (1 - e_M)^{\frac{1}{2}} \cos\omega_M \cos E_f\} -$$

$$3\dot{E}_f \ddot{E}_f\{\sin\omega_M \cos E_f + (1 - e_M)^{\frac{1}{2}} \cos\omega_M \sin E_f\}] , \qquad \text{(A.4.4)}$$

$$\dot{x}_{M_3} = a_M \ddot{E}_f \sin i_M\{-\sin\omega_M \sin E_f + (1 - e_M^{\,2})^{\frac{1}{2}} \cos\omega_M \cos E_f\} -$$

$$a_M \dot{E}_f^{\,2} \sin i_M\{\sin\omega_M \cos E_f + (1 - e_M^{\,2})^{\frac{1}{2}} \cos\omega_M \sin E_f\} ,$$

$$\ddot{x}_{M_3}(t_f) = a_M \cos i_M[(\dddot{E}_f - \dot{E}_f^{\,3})\{-\sin\omega_M \sin E_f + (1 - e_M)^{\frac{1}{2}} \cos\omega_M \cos E_f\} -$$

$$3\dot{E}_f \ddot{E}_f\{\sin\omega_M \cos E_f + (1 - e_M)^{\frac{1}{2}} \cos\omega_M \sin E_f\}] ,$$

$$\dot{E}_f = (\mu/a_M^{\,3})^{\frac{1}{2}} / (1 - e_M \cos E_f) ,$$

$$\ddot{E}_f = \frac{-\dot{E}_f^{\,2} e_M \sin E_f}{1 - e_M \cos E_f} ,$$

$$\dddot{E}_f = \frac{3\ddot{E}_f^{\,2}}{\dot{E}_f} + \ddot{E}_f \dot{E}_f \cot E_f .$$

A4.ii The Tranvenality Condition

The tranvenality condition (2.3.4g) can be written as

$$z(\underline{x}_{t_f}, \underline{u}_{t_f}, t_f, \underline{v}) = [v_1\{(-\frac{\mu x_4}{r^3} + \frac{T}{m}\cos u_1 \cos u_2) - \dot{x}_{M_1}\} + v_2\{-\frac{\mu x_5}{r^3} + \frac{T}{m}\cos u_1 \sin u_2 - \dot{x}_{M_2}\} + v_3\{-\frac{\mu x_6}{r^3} + \frac{T}{m}\sin u_1 - \dot{x}_{M_3}\} + v_4\{x_1 - \dot{x}_{M_4}\} + v_5\{x_2 - \dot{x}_{M_5}\} + v_6\{x_3 - \dot{x}_{M_6}\}]_{t=tf} + \beta \,. \qquad (A.4.5)$$

Using (2.3.3), (2.3.6), and (A.2.1), we have

$$G(\underline{x}_f, t_f, \underline{v}) = \sum_{i=1}^{6} v_i[x_i(t_f) - x_{M_i}(t_f)] \,. \qquad (A.4.6)$$

The Boundary conditions (2.3.19) are then

$$G_{\underline{x}_f \underline{x}_f} = \underset{6\times 6}{0}$$

$$\underline{Y}_{\underline{x}_f} = \underset{6\times 6}{I}$$

$$z_{\underline{x}_f} = -\dot{\underline{\lambda}}_f \qquad (A.4.7)$$

$$\frac{d\underline{Y}}{dt_f} = \dot{\underline{x}}_f - \dot{\underline{x}}_{M_f}$$

$$\frac{dz}{dt_f} = \sum_{i=1}^{n} v_i(\ddot{x}_i - \ddot{x}_{M_i})_{t=t_f}$$

where

$$\ddot{x}_1 = \frac{3\mu x_4}{r^5}[x_4\dot{x}_4 + x_5\dot{x}_5 + x_6\dot{x}_6] - \frac{\mu\dot{x}_4}{r^3} - \frac{T}{m}[\frac{-\beta\cos u_1 \cos u_2}{m}$$

$$+ \sin u_1 \cos u_1 \dot{u}_1 + \cos u_1 \sin u_2 \dot{u}_2]$$

$$\ddot{x}_2 = \frac{3\mu x_5}{r^5}[x_4\dot{x}_4 + x_5\dot{x}_5 + x_6\dot{x}_6] - \frac{\mu\dot{x}_5}{r^3} - \frac{T}{m}[\frac{-\beta\cos u_1 \sin u_2}{m}$$

$$+ \sin u_1 \sin u_2 \dot{u}_1 - \cos u_1 \cos u_2 \dot{u}_2] \qquad (A.4.8)$$

$$\ddot{x}_3 = \frac{3\mu x_6}{r^5}[x_4\dot{x}_4 + x_5\dot{x}_5 + x_6\dot{x}_6] - \frac{\mu\dot{x}_6}{r^3} + \frac{T}{m}[\frac{\beta\sin u_1}{m} + \cos u_1 \dot{u}_1]$$

$$\ddot{x}_4 = \dot{x}_1$$

$$\ddot{x}_5 = \dot{x}_2$$

$$\ddot{x}_6 = \dot{x}_3$$

$$\dot{u}_1 = \frac{-\lambda_3}{\sqrt{\lambda_1^2 + \lambda_2^2}\,(\lambda_1^2 + \lambda_2^2 + \lambda_3^2)}[\lambda_3\lambda_6 + \lambda_2\lambda_5 + \lambda_1\lambda_4] + \frac{\lambda_6}{\sqrt{\lambda_1^2 + \lambda_2^2}}$$

$$(A.4.9)$$

$$\dot{u}_2 = \frac{\lambda_1\lambda_5 - \lambda_2\lambda_4}{(\lambda_1^2 + \lambda_2^2)}$$

APPENDIX 4

FEEDBACK GAIN MATRICES

0.0	-.1721712E 02	0.5335265E 02	-.5645279E 02
	-.2744402E 02	0.3554014E 03	0.2230197E 01
	0.2192804E 00	0.1110709E 01	0.6541234E 00
	0.1081683E 01	0.7964890E 01	-.1128942E -01
6.851333	-.1979636E 02	0.4986687E 02	-.7319661E 02
	-.2489188E 02	0.3175447E 03	0.2176482E 01
	0.7476503E -01	0.1097645E 01	0.5083852E 00
	0.1416520E 00	0.7318948E 01	0.3038645E -03
15.181320	-.2191891E 02	0.4563968E 02	-.9522758E 02
	-.1239404E 02	0.2803958E 03	0.1922581E 01
	-.8750153E -01	0.1050349E 01	0.2624919E 00
	-.6921496E 00	0.6434589E 01	0.1443756E -01
23.681290	-.2298911E 02	0.4168097E 02	-.1197221E 03
	0.9433838E 01	0.2537935E 03	0.1406731E 01
	-.2291337E 00	0.9739190E 00	-.7918924E -01
	-.1173534E 01	0.5510531E 01	0.2828145E -01
32.181290	-.2301952E 02	0.3839275E 02	-.1464174E 03
	0.3921851E 02	0.2392017E 03	0.5498348E 00
	-.3395112E 00	0.8794045E 00	-.5284011E 00
	-.1275840E 01	0.4461711E 01	0.4076630E -01
40.681259	-.2202863E 02	0.3604976E 02	-.1755862E 03
	0.7661143E 02	0.2368889E 03	-.7962586E 00
	-.4141299E 00	0.7790247E 00	-.1103312E 01
	-.1004169E 01	0.3982292E 01	0.5077314E -01
49.181259	-.1990195E 02	0.3491495E 02	-.2078124E 03
	0.1228118E 03	0.2469475E 03	-.2904782E 01
	-.4501182E 00	0.6858255E 00	-.1827065E 01
	-.3609847E 00	0.3555165E 01	0.5621225E -01
57.511230	-.1632689E 02	0.3526346E 02	-.2439881E 03
	0.1806932E 03	0.2692493E 03	-.6220917E 01
	-.4440466E 00	0.6144261E 00	-.2716885E 01
	0.6576290E 00	0.3453117E 01	0.5300790E -01
66.011230	-.1007206E 02	0.3753333E 02	-.2900613E 03
	0.2638577E 03	0.3067588E 03	-.1200906E 02
	-.3836204E 00	0.5762007E 00	-.3888690E 01
	0.2228788E 01	0.3746106E 01	0.3116339E -01
74.511200	0.2094148E 01	0.4244307E 02	-.3582488E 03
	0.4038821E 03	0.3657107E 03	-.2324190E 02
	-.2242206E 00	0.5907142E 00	-.5540355E 01
	0.4820793E 01	0.4561557E 01	-.3691655E -01

83.011200	0.3284534E	02	0.5049292E	02	-.4898533E	03
	0.7181409E	03	0.4616011E	03	-.5097591E	02
	0.2246723E	00	0.6748506E	00	-.8368228E	01
	0.1033583E	02	0.6162663E	01	-.2559355E	00
91.086166	0.1405987E	03	0.4656905E	02	-.8263621E	03
	0.1757207E	04	0.5671111E	03	-.1531651E	03
	0.1891297E	01	0.6401778E	00	-.1477387E	02
	0.2793781E	02	0.8378171E	01	-.1244892E	01
98.736160	0.3030979E	03	-.1501084E	03	-.1688435E	04
	0.7237785E	04	-.7161924E	03	-.8302456E	03
	0.4367702E	01	-.2132745E	01	-.3051900E	02
	0.1205330E	03	-.6778504E	01	-.8982697E	01
107.236130	-.2543965E	04	0.8245547E	03	-.1453970E	04
	0.2259173E	05	-.9735352E	04	-.2679829E	04
	-.4436319E	02	0.9516509E	01	-.2936388E	02
	0.3856045E	03	-.1222640E	03	-.3201256E	02
110.958832	-.5042949E	04	0.2185109E	04	-.1072077E	04
	0.3218859E	05	-.1596482E	05	-.3648477E	04
	-.8801709E	02	0.2664040E	02	-.2467392E	02
	0.5551680E	03	-.2025572E	03	-.4459052E	02
112.064331	-.6051594E	04	0.2759203E	04	-.9398240E	03
	0.3573244E	05	-.1824387E	05	-.3998082E	04
	-.1058064E	03	0.3395969E	02	-.2308005E	02
	0.6184102E	03	-.2323599E	03	-.4926346E	02
115.271774	-.1016523E	05	0.5158129E	04	-.4588318E	03
	0.4865400E	05	-.2652669E	05	-.5259895E	04
	-.1790408E	03	0.6508568E	02	-.1720653E	02
	0.8514036E	03	-.3425264E	03	-.6658400E	02
116.964615	-.1339125E	05	0.7080691E	04	-.1112617E	03
	0.5750163E	05	-.3219469E	05	-.6113547E	04
	-.2372273E	03	0.9054834E	02	-.1284656E	02
	0.1012262E	04	-.4196138E	03	-.7866576E	02
120.020935	-.2222544E	05	0.1243475E	05	0.7905154E	03
	0.7762425E	05	-.4521225E	05	-.8038555E	04
	-.3981309E	03	0.1632336E	03	-.1038910E	01
	0.1384891E	04	-.6017190E	03	-.1068584E	03
123.166077	-.3767869E	05	0.2201906E	05	0.2304918E	04
	0.1036820E	06	-.6233925E	05	-.1047313E	05
	-.6847461E	03	0.2978728E	03	0.1998267E	02
	0.1878582E	04	-.8520857E	03	-.1444788E	03

128.478531	-.7959069E	05	0.4896538E	05	0.6235211E	04
	0.1287280E	06	-.8091100E	05	-.1254069E	05
	-.1491688E	04	0.7033009E	03	0.7977245E	02
	0.2406465E	04	-.1173461E	04	-.1857813E	03
135.437881	-.8540575E	05	0.5475425E	05	0.6424250E	04
	0.2400500E	05	-.1733900E	05	-.2310125E	04
	-.1691168E	04	0.8670313E	03	0.9155713E	02
	0.4691875E	03	-.2858357E	03	-.3812891E	02
139.581573	-.6603163E	05	0.4297975E	05	0.4430723E	04
	-.2993000E	05	0.1754800E	05	0.2630938E	04
	-.1362133E	04	0.7282813E	03	0.6278394E	02
	-.6201250E	03	0.2823750E	03	0.4637108E	02
146.388199	-.4554738E	05	0.3009750E	05	0.2303340E	04
	-.7196000E	05	0.4540900E	05	0.6205063E	04
	-.1022895E	04	0.5792615E	03	0.2779761E	02
	-.1618813E	04	0.8571094E	03	0.1241055E	03
151.806915	-.3921525E	05	0.2603131E	05	0.1515141E	04
	0.9439600E	05	0.6055000E	05	0.7922188E	04
	-.9585271E	03	0.5632852E	03	0.1220947E	02
	-.2316125E	04	0.1287352E	04	0.1779219E	03
157.756897	-.3741444E	05	0.2479950E	05	0.1058488E	04
	-.1221090E	06	0.7856900E	05	0.9910563E	04
	-.1026383E	04	0.6222576E	03	0.4125977E	01
	-.3363438E	04	0.1943938E	04	0.2566482E	03
163.457169	-.3971738E	05	0.2614444E	05	0.8725625E	03
	-.1603060E	06	0.1026250E	06	0.1257488E	05
	-.1248527E	04	0.7722266E	03	-.9259766E	01
	-.5049063E	04	0.3002438E	04	0.3823240E	03
171.107132	-.4841500E	05	0.3143769E	05	0.8295000E	03
	-.2417060E	06	0.1534850E	06	0.1819369E	05
	-.1934359E	04	0.1215016E	04	-.2417577E	02
	-.0672813E	04	0.5874750E	04	0.7165625E	03
176.685242	-.6398000E	05	0.4075100E	05	0.1142750E	04
	-.3614560E	06	0.2262520E	06	0.2616600E	05
	-.3225438E	04	0.2025813E	04	-.3185938E	02
	-.1825081E	05	0.1116506E	05	0.1320000E	04
183.485199	-.1342160E	06	0.8349700E	05	0.4215688E	04
	-.8573440E	06	0.5273920E	06	0.5958200E	05
	-.1017444E	05	-.6304938E	04	0.1250742E	03
	-.6510700E	05	0.3963100E	05	0.4532313E	04

187.248795	-.2375040E	06	0.1448950E	06	0.9092000E	04
	-.1610592E	07	0.9774560E	06	0.1087660E	06
	-.2506600E	05	0.1531500E	05	0.5893125E	03
	-.1695410E		0.1024730E		0.1152700E	

LIST OF REFERENCES

[1] Hart, J. D., "A Comparison of Low-Thrust Guidance Techniques," University of Texas at Austin, Ph.D. Dissertation, 1971.

[2] Lattimore, J. P., "A Comparison of Open and Closed Loop Applications of the Minimum Distance Guidance Technique," University of Texas at Austin, Engineer's Degree Dissertation, 1972.

[3] Wood, L. J., and Bryson, A. E., "Second Order Optimality Conditions for Variable End Time Terminal Control Problems," AIAA/AAS Astrodynamics Conference, Sept. 1972.

[4] Wood, L. J., "Perturbation Guidance for Minimum Time Flight Paths of Spacecraft," AIAA/AAS Astrodynamics Conference, Sept. 1972.

[5] Bryson, A. E. and Yu-Chi Ho, Applied Optimal Control, Blaisdell Publishing Co., Waltham, Massachusetts, 1969.

[6] Wood, L. J., "Second Order Optimality Conditions and Optimal Feedback for Variable End Time Terminal Control Problems," Stanford University, Ph.D. Dissertation, 1972.

[7] Tapley, B. D., and Lewallen, J. M., "Comparison of Several Numerical Optimization Methods," Journal of Optimization Theory and Applications, Vol. 1, No. 1, 1967.

[8] Williamson, W. E. and Tapley, B. D., "Riccati Transformations for Control Optimization Using the Second Variation," AMRL 1035, University of Texas at Austin, 1971.

[9] Bulirsch, R., and Stoer, J., "Numerical Treatment of Ordinary Differential Equations by Extrapolation Methods," Numerische Mathematik 8, p. 1-13, 1966.

[10] Powers, W. F., "A Method for Comparing Trajectories in Optimum Linear Perturbation Guidance Schemes," AIAA Journal, Vol. 6, No. 12, pp. 2451-52, December 1968.

[11] Speyer, J. L., and A. E. Bryson, "A Neighboring Optimum Feedback Control Scheme Based on Estimated Time-To-Go with Application to Re-Entry Flight Paths," AIAA Journal, Vol. 6, No. 5, pp. 769-76, May 1968.

[12] Irving, J. H., Space Technology, John Wiley and Son, Inc., New York, 1959, Chapter 10.

[13] Powers, W. F., "Techniques for Improved Convergence in Neighboring Optimum Guidance," AIAA Journal, Vol. 8, No. 12, pp. 2235-41, December 1970.

[14] Wood, L. J., private communication, March 1975, Hughes Aircraft Company, El Segundo, California.